8-8-2007

An Improved Model for Estimating Evaporation over Lakes and Ponds

Ravi Praveen Eluripati
University of New Orleans

An Improved Model for Estimating Evaporation over Lakes and Ponds.

A Thesis

Submitted to the Graduate Faculty of the
University of New Orleans
in partial fulfillment of the
requirements for the degree of

Master of Science
in
The Department of Mechanical Engineering

by

Ravi Praveen Srinivasa Eluripati

B.E., Osmania University, 1999

August 2007.

ACKNOWLEDGEMENTS

I am highly indebted to Dr. Carsie A. Hall, III, major professor and graduate advisor, for his guidance and inspiration that assisted me towards a successful completion of my thesis. I would like to express my sincere appreciation and gratitude for his coordination via classes and invaluable suggestions during the entire period. I have a special thanks to Dr. Hall for providing me financial support during my graduate study at University of New Orleans.

Next, I would like to thank Dr. Edwin P. Russo for his support during my thesis-research. His extensive support with literature search, thesis work review and his productive and informative discussions has greatly helped me to complete my thesis.

I would also thank Dr. Martin J. Guillot for serving as a committee member in my thesis defense despite his extremely busy schedule.

To my parents, brother and sister, to whom I dedicate this work, I express a most appreciative thank you for their love and encouragement during the entire period that has made this work possible.

Last and not the least, I extend a special thanks to all my friends and colleagues for supporting me and encouraging my work.

TABLE OF CONTENTS

page

ABSTRACT ..... **VIII**

NOMENCLATURE ..... **IX**

CHAPTER 1: INTRODUCTION **1**

1.1 FACTORS EFFECTING EVAPORATION 1

1.2 IMPORTANCE OF EVAPORATION KNOWLEDGE 2

CHAPTER 2: LITERATURE REVIEW **3**

2.1 LAKE HEFNER EVAPORATION MODEL 3

2.2 HOLMAN'S EVAPORATION FORMULA 4

2.3 MODIFIED HOLMAN'S FORMULAE IN AMBIENT AIR TEMPERATURE AND RELATIVE HUMIDITY 5

2.4 EPRI MODEL – REPORT NO.14 – EVAPORATION MODEL 7

2.5 EVAPORATION EQUATION FROM SOLAR ENGINEERING FOR DOMESTIC BUILDINGS 7

2.6 ASHRAE HANDBOOK, 1999 8

CHAPTER 3: FUNDAMENTALS OF EVAPORATION **9**

3.1 WATER COLUMN 9

3.2 ATMOSPHERIC AND SOLAR RADIATION FUNDAMENTALS 13

3.3 SOLAR CONSTANT 13

3.4 DIRECT AND DIFFUSE SOLAR RADIATION 14

3.5 SOLAR ATTENUATION IN ATMOSPHERE 17

3.6 SCATTERING OF ENERGY BY PARTICLES 21

3.7 RAYLEIGH SCATTERING: 23

3.8 MIE SCATTERING: 23

3.9 HEAT EXCHANGE AT WATER SURFACE 24

3.9.1 Short Wave Solar Radiation (H_s): *27*

3.9.2 Long Wave Atmospheric Radiation (H_a): *28*

3.9.3 Reflected Solar and Atmospheric Radiation (H_{sr} and H_{ar}): *30*

3.9.4 Long wave Back Radiation (H_b): *30*

3.9.5 Conduction Heat Loss or Gain (H_c): *31*

3.9.6 Evaporation (H_e): *31*

CHAPTER 4: PROPOSED ENERGY BALANCE MODEL 33

4.1 CONDUCTION ZONE 33

4.2 SOLAR ENERGY RADIATION 35

4.3 CLOUD COVER 35

4.4 SOLAR ENERGY ABSORPTION IN WATER 38

4.5 SOLAR RADIATION RELATION AS A FUNCTION OF TIME OF DAY 43

4.6 SKY RADIATION 45

4.7 SKY RADIATION / CLOUD COVER 48

4.8 CLOUDS 50

4.9 WATER SURFACE TEMPERATURE 52

4.10 EVAPORATION 54

4.11 CONVECTION 55

4.12 ENERGY BALANCE ANALYSIS 56

CHAPTER 5: RESULTS AND CONCLUSION..... 58

5.1 LAKE HEFNER EVAPORATION MODEL..... 58

5.2 JP HOLMANS EVAPORATION FORMULA – IN VAPOR PRESSURES 59

5.3 JP HOLMAN'S FORMULA MODIFIED USING AMBIENT TEMPERATURE 60

5.4 EPRI MODEL – REPORT NO.14 – EVAPORATION MODEL 61

5.5 EVAPORATION EQUATION FROM SOLAR ENGINEERING FOR DOMESTIC BUILDINGS 62

5.6 ASHRAE HANDBOOK, 1999..... 63

5.7 ENERGY BALANCE MODEL 64

5.8 COMPARISON OF ALL MODELS 65

REFERENCES..... 67

VITA 69

LIST OF FIGURES

FIGURE 1 - TYPICAL NEAR-SURFACE TEMPERATURE PROFILES ILLUSTRATING THE DIURNAL THERMOCLINE IN CALM, SLIGHTLY MIXED AND NIGHTTIME CONDITIONS 11

FIGURE 2 - VERTICAL PROFILES OF OCEAN TEMPERATURES AT DIFFERENT LATITUDES 12

FIGURE 3 - DIRECT AND DIFFUSE SOLAR RADIATION 15

FIGURE 4 - ABSORPTION AND SCATTERING OF SOLAR RADIATION 16

FIGURE 5 - SPECTRAL DISTRIBUTION OF SOLAR RADIATION ON A TYPICAL DAY 19

FIGURE 6 - ELECTRONIC WAVE TRANSMITTANCE AS A FUNTION OF WAVELENGTH 20

FIGURE 7 - PHYSICAL PROCESSES INFLUENCING AN AIR-WATER INTERFACE 25

FIGURE 8 - PROCESSESS OF HEAT EXCHANGE AT NATURAL WATER SURFACE 26

FIGURE 9 - BRUNT'S COEFFICIENT 29

FIGURE 10 - THERMODYNAMIC AIR-WATER INTERFACE ZONES 34

FIGURE 11 - REFLECTIVITY OF SOLAR RADIATION 37

FIGURE 12 - MEAN DAILY SOLAR RADIATION AS A FUNTION OF MONTH 44

FIGURE 13 - ATMOSPHERIC RADIATION FACTOR AS A FUNCTION OF VAPOR PRESSURE AND CLOUD COVER 49

FIGURE 14 - SATELLITE SENSOR MEASUREMENT 53

LIST OF TABLES

TABLE 1 - FRACTION OF SOLAR RADIATION SPECTRUM TRANSMITTED THROUGH VARIOUS THICKNESS OF WATER. 39

TABLE 2 - FRACTIONS OF SOLAR RADIATION SPECTRUM ABSORBED IN VARIOUS WATER LAYERS 40

TABLE 3 - ANGLE OF REFRACTION R, REFLECTIVE LOSS, AND 1/COS R FOR VARIOUS ANGLES OF INCIDENCE 42

TABLE 4 - SKY EMISSIVITY 47

TABLE 5 - EFFECTS OF CLOUDS 50

TABLE 6 - STRUCTURE OF THE ATMOSPHERE 51

ABSTRACT

The objective of this study is to develop an improved method for calculating the evaporative energy that is being transferred from the surface of a pond or lake to the surrounding atmosphere. The energy balance method developed in this study is based on the equations, assumptions and empirical relations for conductive, convective and radiative energies that are developed by various researches at the air-water interface conducted in the past. This method is then tested with field data for verifying its correctness. The experiment was conducted on a 200-meter diameter and 9 meter deep fresh water pond. Water temperatures were measured at the surface and at 2.5, 10, and 50 centimeters below the surface. Solar and sky radiation were recorded on nearby land based optical pyronameters. The following thesis is a careful study of the several published research methods in comparison with the energy-balance method.

NOMENCLATURE

E = evaporation rate, m/s

E' = evaporation rate, inches/day

G_s = solar constant, W/m^2

h = convective heat transfer coefficient, $W/(m^2\text{-}K)$

h_{fg} = latent heat of vaporization, J/kg

h_r = radiative heat transfer coefficient, $W/(m^2\text{-}K)$

k = water thermal conductivity, $W/(m^2\text{-}K)$

L = distance between earth and sun, m

p_s = saturation vapor pressure at dry-bulb air temperature, N/m^2

p_s' = saturation vapor pressure at dry-bulb air temperature, inches of Hg or mb

p_w' = actual vapor pressure of air under air temperature and humidity conditions, inches of Hg or mb

Q_{conv} = convective heat transfer, W/m^2

Q_D = direct solar radiation, W/m^2

Q_d = diffuse solar radiation, W/m^2

Q_{evap} = evaporative heat transfer to air, W/m^2

Q_{rad} = radiative heat transfer to sky, W/m^2

Q_{sky} = radiative heat transfer from sky, W/m^2

Q_{solar} = solar radiation, W/m^2

Q_{water} = conductive heat transfer from water bulk, W/m^2

R = radius of the sun, m

t = time, hours

T_{air} = air temperature, K

T_{dew} = dew point temperature, °C

T_m = mean temperature of T_s and T_{sky}, K

T_s = water surface temperature, K

T_{sky} = effective sky temperature, K

T_{sun} = temperature of the sun, K

T_w = bulk water temperature, K

u = wind speed, miles/day

V = wind speed, m/s

$\forall$ = water absorptivity of infrared sky radiation

$\forall_s$ = water absorptivity of solar radiation

Φ = Stefen-Boltzmann constant, $W/(m^2\text{-}K^4)$

N = relative humidity

δ = Conduction zone thickness, m

ρ_{Water} = water density, kg/m^3

θ = angle of incidence of solar radiation, degrees

ε = water emissivity

ε_{Sky} = sky emissivity

μ = Micro = 10^{-6}

CHAPTER 1: INTRODUCTION

The dynamics of air – water interface is extremely complicated and not well understood phenomenon. There has been constant research in this field to understand this concept much clearly. The ambiguity in this concept can be related to the simultaneous heat & mass transfer, including conduction, convection, radiation, and vaporization of the water known as evaporation. The evaporation process is complicated because atmospheric convection currents that are difficult to describe analytically govern it. The energy required to sustain the evaporation must come from the internal energy of water. The energy transfer to the liquid from its surroundings replenishes the latent energy lost by the liquid due to evaporation. This transfer may be due to solar radiation or convection of sensible energy from the air.

1.1 FACTORS EFFECTING EVAPORATION

Evaporation is the process of heat and mass transfer from a water body to the surrounding which produces a net cooling effect on the water body. The effect of evaporation can be observed as reduction of temperature of the water body. There are two driving forces for evaporation, which are:

1. Concentration gradient
2. Turbulent diffusion and convection transport

A concentration gradient is created due to the vapor pressure difference between the saturated vapor pressure at the air-water interface and the water vapor pressure of the overlying air above the air-water interface.

The later driving force causes evaporation when the liquid molecules at the water surface experience collisions that increases the internal energy of the water molecules above their surface binding energy and hence causes the molecule to liberate itself into the air. The energy in

such a process comes from the water body itself and the loss of energy associated due to evaporation can be seen as drop in the water temperature.

Observation have shown that on a normal day and under normal wind speed and ambient conditions, evaporation due to turbulent diffusion and convection transport is at least 1000 times higher than molecular diffusion.

1.2 IMPORTANCE OF EVAPORATION KNOWLEDGE

The knowledge of evaporation is helpful in conducting water budget studies for preserving water resources and planning water consumption which is one of the most important natural resources. The knowledge about evaporation is also helpful in commercial remote sensing applications to forecast weather and natural calamities such as cyclones and thunderstorms by detecting the formation of low-pressure and high-pressure regions due to evaporation. Power plant applications often use water-cooled condensers to condense steam into water by using river water as the medium for heat exchange. The knowledge of evaporation helps us to understand the impact of the temperature change of the river water and take measures to protect the local ecological system.

CHAPTER 2: LITERATURE REVIEW

As literature survey, various evaporation models developed by many researchers in the past have been considered by this study. Six models have been discussed in detail in the following sections of this chapter. All these models explained below and the model proposed later on as result of this research study have been analyzed using real-time data obtained from experiments. The results of the analysis have been discussed in Chapter 4.

2.1 LAKE HEFNER EVAPORATION MODEL

Lake Hefner aerodynamic equation for evaporation (in inches/day):

$$E_p = (e_0 - e_a) * (0.42 + 0.0040 u_p)$$

where, e_0 = Saturation vapor pressure of the air (in HgA)

e_a = Vapor pressure of ambient air lying much above the water surface (in HgA)

u_p = Wind movement or speed (in miles / day)

Evaporation Heat Flux (W/m^2):

$$Q_{evap} = E_p * \rho * h_{fg}$$

where, E_p = Evaporation (in meters/second)

ρ = density of water (1000 kg/m^3)

h_{fg} = Latent heat of vaporization (2,450,000 J/kg)

Conversions needed:

1 Kpa = 0.2952999 in HgA

1 meter/second = 3,401,573.76 inches/day

1 meter/second = 53.6864733 miles/day

2.2 HOLMAN'S EVAPORATION FORMULA

A general evaporation formula may be expressed as the product of a wind function, f(V) and the difference between the saturated water vapor pressure; p_w, at the water surface temperature and the water vapor pressure, p_a, in the air above the water, that is

$$Q_{evap} = f(V)(p_w - p_a)$$

with

$$f(V) = C_1 + C_2 V + C_3 V^2 + ...$$

where V is the long-term average wind speed in meters/second and C_n's are coefficients. It should be noted that this relation predicts evaporative heat flow in the absence of wind, i.e., calm conditions. This is not to be confused with molecular diffusion type of evaporation, which is negligible in comparison with the turbulent/convection type of environmental evaporation as given above. The existence of weak vertical currents, above and below the water surface, caused by density instabilities will contribute to evaporation rates in the absence of wind (Harbeck, 1969).

Holman (1986) introduces the following empirical experimental formulae for the evaporation rate (E') from ponds and lakes (Kohler, et al, 1955)

$$E' = 0.8(0.37 + 0.0041u)(p'_s - p'_w)^{0.88}$$

where, u = daily wind movement, miles/day

p'_s = saturation vapor pressure at dry-bulb air temperature, inches of Hg

p'_w = actual vapor pressure of air, inches of Hg

The 0.8 factor in the equation is to account for the floating pan as opposed to a land pan (0.7).

2.3 MODIFIED HOLMAN'S FORMULAE IN AMBIENT AIR TEMPERATURE AND RELATIVE HUMIDITY

The equation (2.2.3) above is converted to SI units to make the equation applicable to the data recorded in SI units.

$$E = \frac{E'(inches/day)}{24(hrs/day)3600(\sec s/hr)39.37(inches/meter)}$$

or

$$E = \frac{E'}{3{,}401{,}568}$$

The wind speed term must be converted from miles/day to meters/second, thus

$$V = \frac{U(miles/day)1609(meters/mile)}{24(hrs/day)3600(\sec s/hr)}$$

or

$$V = 0.0186u$$

The pressure term may be written in terms of relative humidity, φ, namely

$$\left(p_s' - p_w'\right)^{0.88} = \left(p_s' - \varphi p_s'\right)^{0.88} = \left(p_s'(1-\varphi)\right)^{0.88}$$

The pressure must be converted to SI units, N/m^2 (i.e., pascals)

p'_s [inches of Hg] = $2.953 \times 10^{-4} p_s$ [N/m^2]

Hence Equation 2.2.3 can now be written in SI units as,

$$E = \frac{0.8\left(0.37 + \frac{0.0041V}{0.0186}\right)\left(2.953*10^{-4}\, p_s'(1-\varphi)\right)^{0.88}}{3{,}401{,}575}$$

or

$$E = 1.84 * 10^{-10}\left(0.37 + 0.22V\right)\left(p_s\left[1-\varphi\right]\right)^{0.88}$$

This formula may be converted into heat flow as follows

$$Q_{evap} = E\left(\frac{Meters}{Second}\right)\rho\left(\frac{Kgs}{m^3}\right)h_{fg}$$

noting that Joule per second (i.e., J/s) equals to Watt (i.e., W). The average values for density (1000 kg/m^3) and latent heat of vaporization (i.e., 2,450,000 J/kg) can be used in the above equation, which changes the equation as,

$$Q_{evap} = E\left(1000\right)\left(2{,}450{,}000\right)$$

or

$$Q_{evap} = 0.45\left(0.37 + 0.22V\right)\left(p_s\left[1-\varphi\right]\right)^{0.88}$$

The vapor pressure, p'_s, may be eliminated from the above equation in favor of a more conveniently measured variable, namely T_{air}, thus eliminating the need for steam table "look-ups". Hall and Mackie (2000) gave the following expression for p_s in terms of T_{air} for temperatures in the ranges of the typical air values (i.e., 10^o C to 40^o C), that is

$$P_s = 5T_{air}^2 - 51T_{air} + 1282$$

Thus, the heat evaporation equation may be re-written as,

$$Q_{evap} = 0.45\left(0.37 + 0.22V\right)\left(5T_{air}^2 - 51T_{air} + 1282\right)^{0.88}\left(1-\varphi\right)^{0.88}$$

The above equation has been used with the available data for evaluating the applicability of the evaporation model.

ADVECTION

The energy lost by the physical removal of heat contained in the water removed by evaporation is given by

$$Q_{advected} = E\rho c\left(T_{water} - T_{base}\right)$$

where c is the specific heat of water (i.e., 4178 J/[kg.K] in SI units) and T_{base} is taken to be 0 degrees Celsius. Therefore,

$$Q_{advected} = 0.00077\left(0.37 + 0.22V\right)\left(p_s\left[1-\varphi\right]\right)^{0.88}$$

2.4 EPRI MODEL – REPORT NO.14 – EVAPORATION MODEL

Evaporation equation prepared for Electric Power Research Institute, Report no.14 (Edinger, et al., 1974) in W/m^2 is given as,

$$E = \left(9.2 + 0.46W^2\right)\left(e_s - e_a\right)$$

where, W = wind speed at a height of 7m above the water surface (meters/second)

e_s = Saturation vapor pressure of air (mm HgA)

e_a = Vapor pressure of ambient air lying above the water surface (mm HgA)

Conversions needed

1 Kpa = 7.500617 mm HgA

2.5 EVAPORATION EQUATION FROM SOLAR ENGINEERING FOR DOMESTIC BUILDINGS

Evaporation losses from pools as given by Himmelman, 1980 [W/m^2],

$$Q_{evap} = 9.15K_E\left(e_s - e_a\right)$$

where,

K_E = Convective heat transfer coefficient varying from 1.36 $(\Delta T)^{0.25}$ for still air to

about 23 W/m^2.°C for an air velocity of 4.5 meters/second.

e_s = Saturation vapor pressure of air (mbar)

e_a = Vapor pressure of ambient air lying above the water surface (mbar)

Assumed value for K_E,

K_E = 60 W/m^2.°C (Suggested value from ASHRAE Handbook, 1999)

Conversions needed

1 Kpa = 10 mbar

2.6 ASHRAE HANDBOOK, 1999

Heat Loss from a swimming pool surface in Btu/hr.ft^2 is given as,

$$Q_{evap} = WU\left(T_p - T_a\right)$$

where, W = Wind speed correction factor obtained from the following equation

$$W = -2.82051E-02x^2 + 5.73077E-01x - 9.10256E-01$$

where x is the actual wind speed in meters/second. (This equation is developed from the absolute factors and absolute wind speed values at three different points.)

U = surface heat transfer coefficient = 10.5 Btu/hr.ft^2.°F (1.75099 W/m^2.°C)

T_p = Water surface temperature (°F)

T_a = Air Temperature (°F)

Conversion used:

1 Btu/hr.ft^2 = 3.1517849 W/m^2

CHAPTER 3: FUNDAMENTALS OF EVAPORATION

3.1 WATER COLUMN

The temperature variation in a deep-water body may be explained as follows. The ocean is heated from the above by solar/atmospheric heating and the warmer water being less dense than cooler causes the ocean temperature to decrease with depth. However, there is a surface layer that extends from a few meters to several hundreds of meters, which is essentially uniform. Below this layer, the temperature decreases rapidly, which is called the thermo-cline. Figure 1 shows a typical sea surface at different latitudes that exhibit different sea surface layer and thermo-cline characteristics. It can be seen from Figure 2 that temperature decreases very little and is approximately the same at most latitudes. (Robinson, 1997).

The potential for stratification of the surface layer by penetration of the solar radiation tends to be balanced by wind induced mixing, and by vertical convection as a result of water cooling at the surface and sinking. This balance establishes a vertically homogeneous upper layer, which continually exchanges heat with the atmosphere via energy from sky atmospheric radiation and loss of energy by convection, evaporation, and radiation from the water. If solar radiation were the only heating mechanism in the upper layers of the water column, the temperature would follow an exponential decay (Edinger, et al, 1974).

Both wind conditions and solar radiation show a strong seasonal variation and hence the water column too will reflect these seasonal variations. Figure 1 shows the effects of seasonal variations and diurnal (day/night) effects on a sea surface. In summer, wind mixing is generally less and solar heating is increased thus creating a shallow mixed layer which is also the same case with a calm sunny day as shown in Figure 2; whereas, in the winter there will be a high wind mixing, which causes a deeper mixed layer at low temperature. Both seasonal variations

and diurnal variation have been observed to have a significant effect on sea surface conditions and must be considered for any study of this kind. Solar heating causes the surface temperature to increase locally above the upper mixed temperature and this effect will be very weak if there is significant wind-mixing (Edinger, at al, 1974). The surface water becomes heavier and sinks, promoting mixing, which destroys the diurnal thermocline quite rapidly after sunset due to the absence of solar radiation.

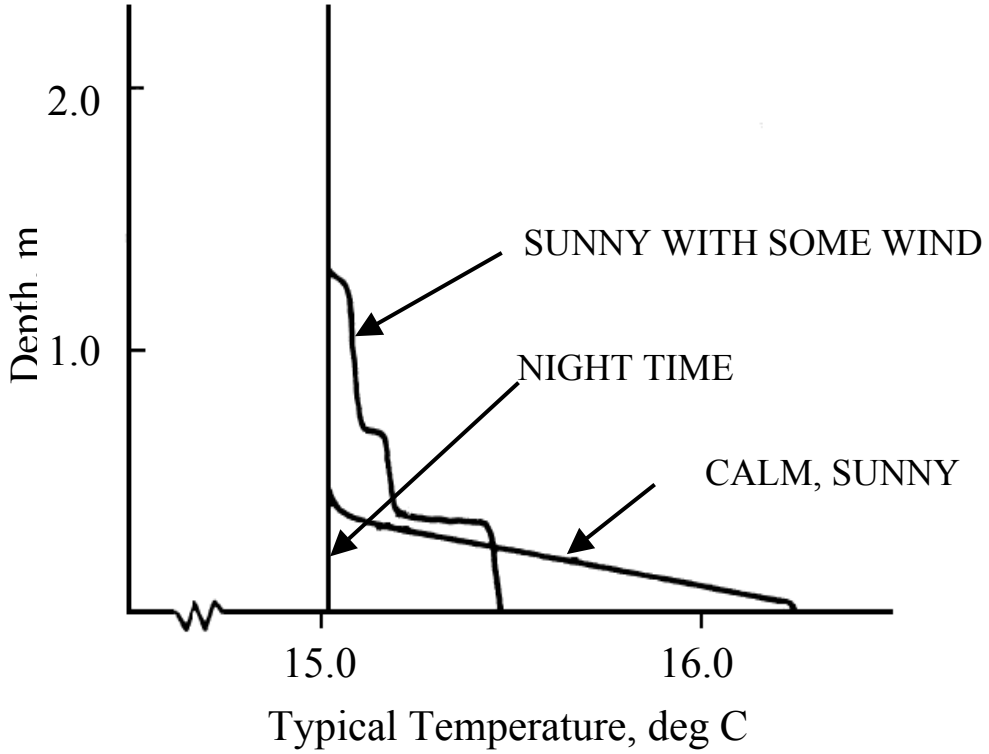

FIGURE 1 - TYPICAL NEAR-SURFACE TEMPERATURE PROFILES ILLUSTRATING THE DIURNAL THERMOCLINE IN CALM, SLIGHTLY MIXED AND NIGHTTIME CONDITIONS

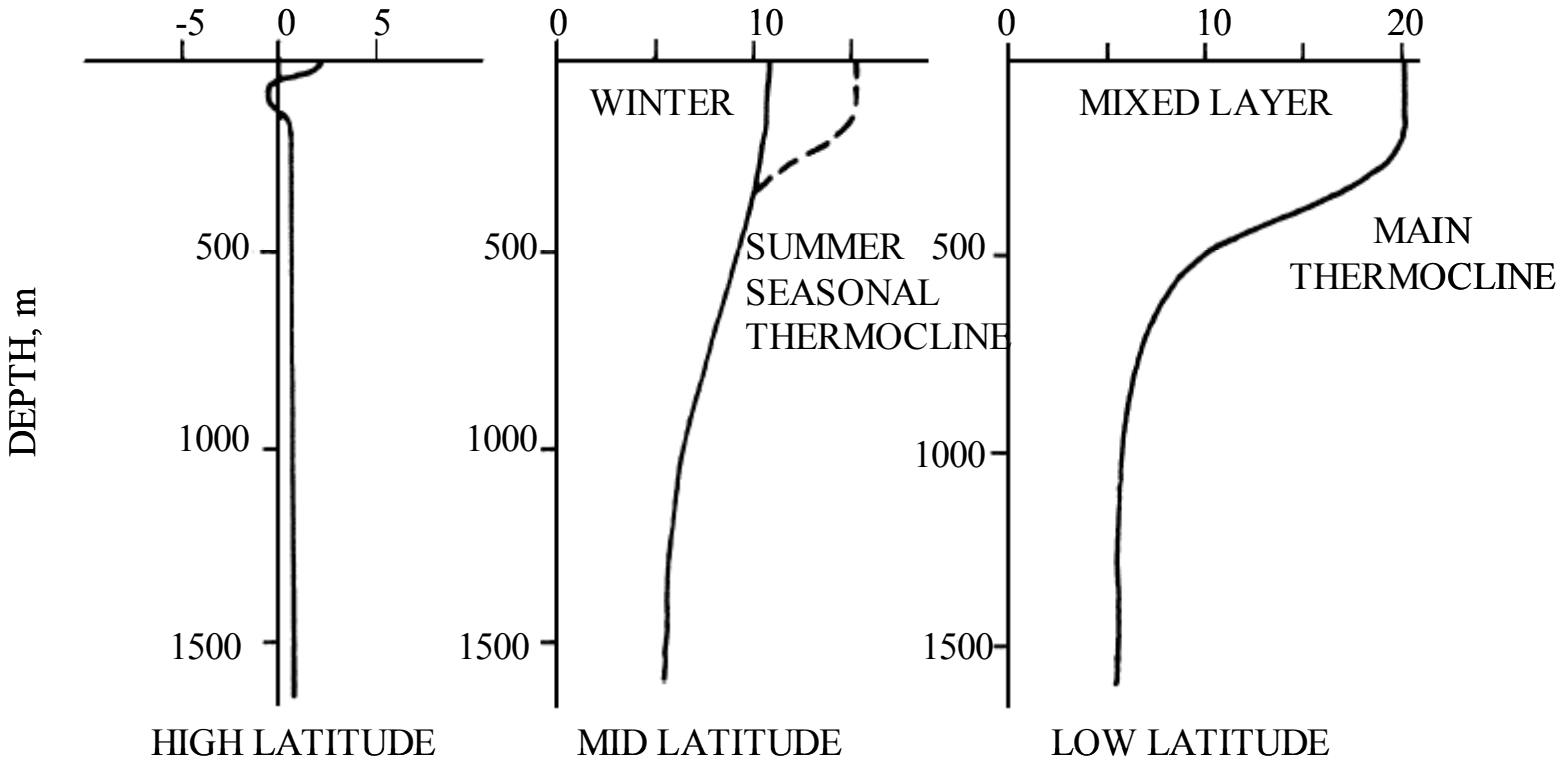

FIGURE 2 - VERTICAL PROFILES OF OCEAN TEMPERATURES AT DIFFERENT LATITUDES

3.2 ATMOSPHERIC AND SOLAR RADIATION FUNDAMENTALS

The sun is nearly spherical body that has a diameter of 1.39×10^6 kilometers and is located at a mean distance of 1.5×10^8 kilometers from the earth. It emits radiation energy continuously at a rate of approximately 4×10^{23} kilowatts. Less than a billionth of this energy (about 2 x 10+14+ kilowatts) strikes the earth. The sun is essentially a nuclear reactor with temperatures as high as 40,000,000 K in its core region. The temperature drops to about 5800 K in its outer region of the sun.

3.3 SOLAR CONSTANT

The solar energy reaching the outer edge of the earth's atmosphere is called solar constant, G_s. The solar constant represents the rate at which solar energy is incident on a surface normal to the sun's rays at the outer edge of the atmosphere, when the earth is at its mean distance from the sun. The actual value of the solar constant varies throughout the year owing to the ellipticity of the earth's orbit. It varies from a minimum of 1310 W/m^2 on June 21 to a maximum of 1399 W/m^2 on December 21. However, this variation (which is ± 3 percent of the mean value) is considered negligible for most engineering purposes, and thus G_s may be taken to be a constant at its mean value of 1353 W/m^2 (Cengel, 1998).

The Solar constant can be used to estimate an effective surface temperature of the sun by noting that the total solar energy passing through a spherical surface whose radius is the mean earth-sun distance must be equal to the total energy that leaves the sun's outer surface, that is

$$(4\pi S^2)\, G_s = (4\pi R^2)\, \sigma\, T^4_{sun}$$

where R is the radius of the sun and S is the mean distance between centers of sun and earth. The effective surface temperature of the sun may be determined from the above equation to be T_{sun} =

5762 K. That is, the sun can be treated as a black body at a temperature of 5762 K (Cengel, 1998).

3.4 DIRECT AND DIFFUSE SOLAR RADIATION

The previous section explains about Solar Constant which is the solar energy reaching the earth's outer atmosphere. This radiation is considered to reach the surface of the earth as direct solar radiation and diffuse solar radiation. Figure 3 represents the direct and indirect radiation incident on a horizontal surface at the earth's surface. The part of radiation that reaches the earth's surface without being scattered or absorbed by the atmosphere is called direct solar radiation, Q_D. The scattered radiation is assumed to reach the earth's surface uniformly from all directions on the unit area of a horizontal surface as shown in Figure 4. Hence the total solar energy incident on a unit area of a horizontal surface is calculated as:

$$Q_{solar} = Q_D \cos \theta + Q_d \ (W/m^2)$$

where θ is the angle of incidence of direct solar radiation (i.e., the angle that the sun's rays make with the normal to the surface). The diffuse radiation varies from about 10 percent of the total radiation on a clear day to nearly 100 percent on a totally cloudy day (Cengel, 1998).

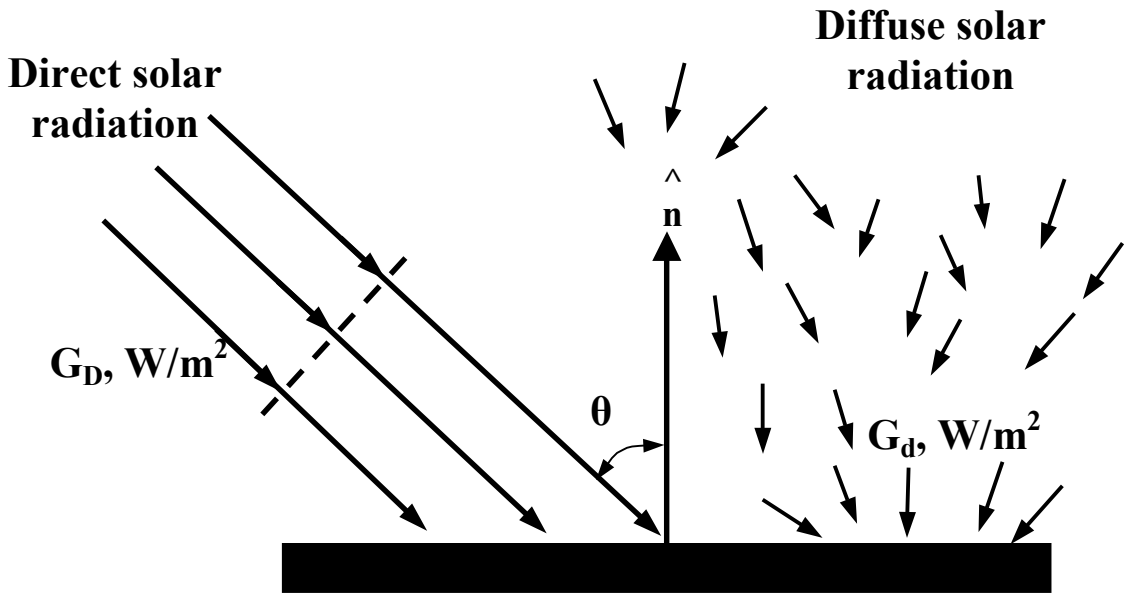

FIGURE 3 - DIRECT AND DIFFUSE SOLAR RADIATION

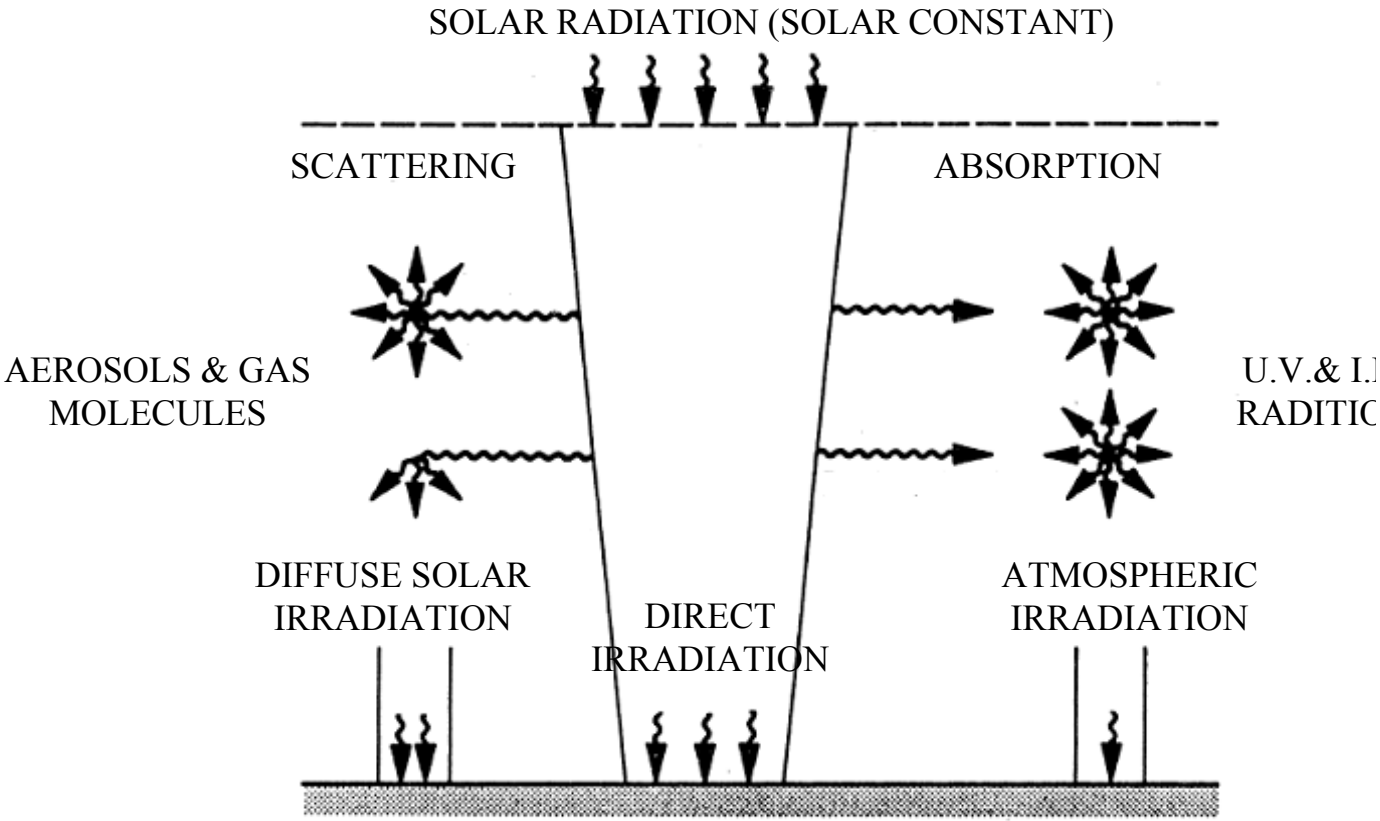

FIGURE 4 - ABSORPTION AND SCATTERING OF SOLAR RADIATION

3.5 SOLAR ATTENUATION IN ATMOSPHERE

The energy coming from the sun reaches the earth in the form of electromagnetic waves after experiencing considerable interactions with the atmosphere. The radiation energy emitted or reflected by the constituents of the atmosphere form the atmospheric radiation. The spectral distribution of the solar radiation on the surface of the earth as depicted in Figure 5 explains that the solar radiation undergoes considerable attenuation as it passes through the atmosphere as a result of scattering and absorption. Weiss (1971) notes that atmospheric radiation is nearly linear with altitudes up to 2000 meters. A typical transmission spectrum for the atmosphere is given in Figure 6 (Reeves, 1975). This figure explains that the atmosphere absorbs most radiation with wavelengths less than 0.3μm and much above 1μm. There is a definite window in the visible range and also in selected bands within the infrared. These bands have been exploited for remote sensing (Robinson, 1997). Between 20μm and 1000μm there is more absorption, but above there is very little absorption. The dips on the spectral distribution of radiation on the earth's surface are due to absorptions by gases O_2, O_3 (ozone), H_2O (water vapor), and CO_2 (carbon dioxide). Absorption by O_2 (oxygen) occurs in a narrow band about wavelength 0.76 μm. The ozone, O_3, absorbs ultraviolet radiation at wavelengths below 0.3μm almost completely, and radiation in the range 0.3 – 0.4 μm considerably. The ozone gas also absorbs some radiation in the visible range (0.4 – 0.7 μm) and in the 9 μm to 10 μm range of the thermal infrared. To avoid the effects of the O_3 absorption satellite IR sensors use the 10 μm to 12 μm range; whereas, aircraft systems which fly beneath the ozone layer use the full 8 μm to 14 μm window for recording. Absorption in the infrared region is dominated by water vapor and carbon dioxide. As a result of these absorptions, the solar energy reaching the earth's surface is reduced to about 900 W/m^2 on a clear day and much less on cloudy days. The average annular solar irradiation for the entire earth's surface is

given as 172 W/m^2 by Kreith and Kreider (1978). Practically all of the solar radiation reaching the earth's surface falls in the wavelength band from 0.3 to 2.5 μm (Cengel, 1998)

.

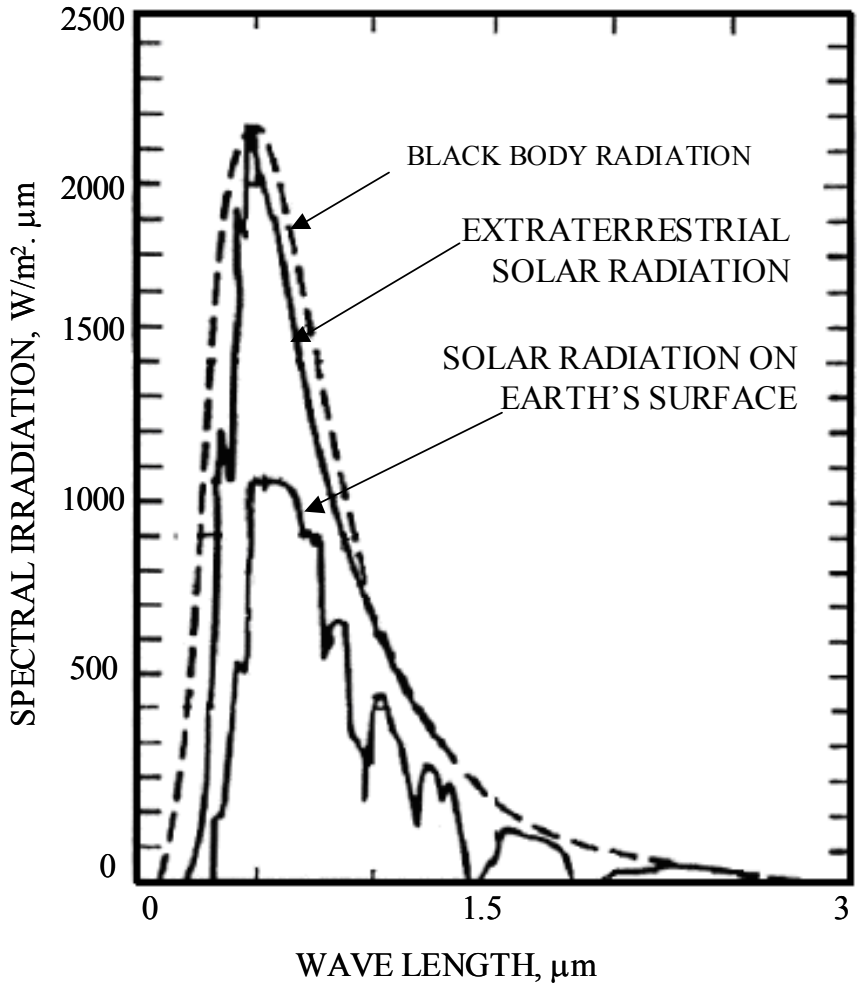

FIGURE 5 - SPECTRAL DISTRIBUTION OF SOLAR RADIATION ON A TYPICAL DAY

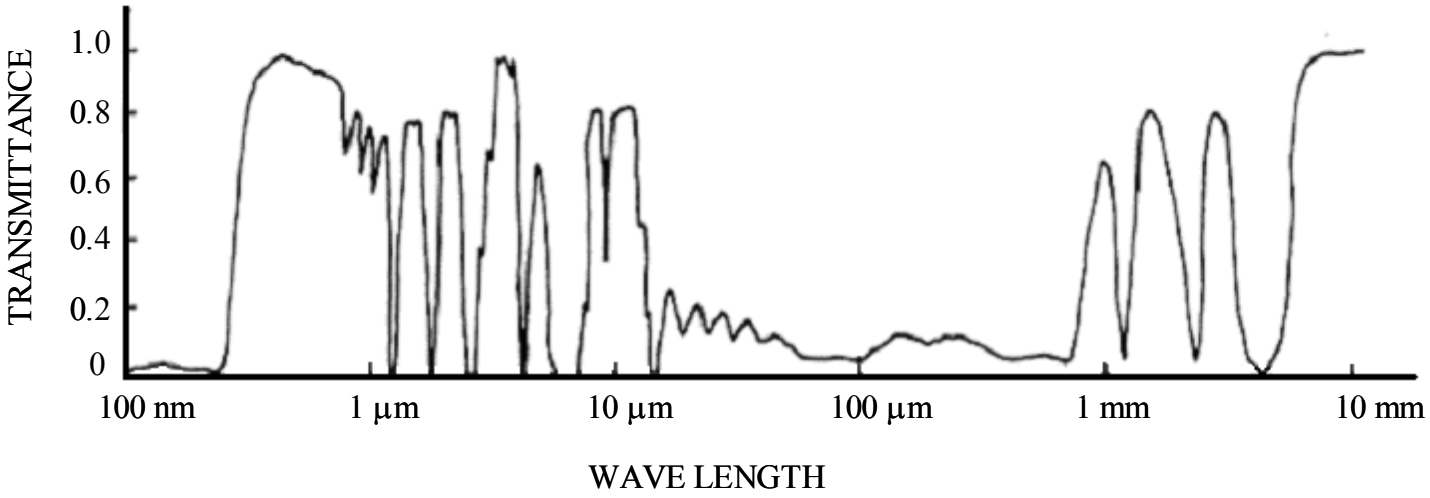

FIGURE 6 - ELECTRONIC WAVE TRANSMITTANCE AS A FUNTION OF WAVELENGTH

3.6 SCATTERING OF ENERGY BY PARTICLES

Scattering is an encounter between a photon and one or more other particles during which the photon does not lose its entire energy. It may undergo a change in direction and a loss or a gain of energy. The scattering coefficient $\sigma_{s\lambda}$ is the inverse of the mean free path that a photon of wavelength λ will travel before undergoing scattering (strictly true only when $\sigma_{s\lambda}$ does not vary along the path). Scattering can be characterized by four types of events:

a. *Elastic* scattering in which the energy (and, hence, frequency and wavelength) of the photon is unchanged by scattering.
b. *Inelastic* scattering in which the energy is changed.
c. *Isotropic* scattering in which scattering into any direction is equally likely, and
d. *Anisotropic* scattering in which there is a distribution of scattering directions.

Elastic-isotropic scattering is most amenable to analysis. In addition, most scattering of engineering importance is essentially elastic (Siegel and Howell, 1992).

When incident radiation strikes a particle, some of the incident radiation may be reflected from the particle surface. The remaining radiation will penetrate into the particle, where part can be absorbed. If the particle is not a strong internal absorber, some of this radiation will leave. This may occur after travel along a single path through the particle, or radiation may undergo multiple internal reflections before escaping. When interacting with the particle boundary, the radiation will be refracted and will have its direction changed by subsequent internal reflections. The redirection by these processes of the energy penetrating into the particle and then escaping is *scattering by refraction*.

Additional scattering is by *diffraction*, which produces the interference patterns observed when light passes through an aperture in a screen. Diffraction is the result of slight bending of the radiation path passing near the edges of an obstruction.

For a process with elastic scattering and without emission or absorption, there is no exchange of energy between the radiation field and the medium. Hence, the radiation field does not affect the thermodynamic conditions of the medium. Scattering calculations for this special case are more tractable than when the internal energy of the medium and the radiation field interact by absorption and emission.

A common simplification is to let the scattering particles have the properties of spheres. This is assumed so because in any ransom orientation, an equal portion of surface elements will face each angular direction. The interaction of electro magnetic waves with a particle produces scattering by reflection, refraction and diffraction, and these effects depend on two parameters containing the particle properties and size. An important property of a particle that affects scattering is its index of refraction, an optical property of the particle relative to surrounding medium. The second important parameter is the particle size relative to the wavelength λ_m of the radiation within the particle. This is usually expressed as a size parameter $\xi = \pi D/\lambda_m$ where D is the spherical particle diameter. The scattering behavior of a particle varies significantly with the size of the particle which is expressed in terms of ξ. For large spheres, ξ greater than about 5, the scattering is chiefly a reflection process and can be calculated from relatively simple geometric reflection relations. There is a also diffraction of radiation passing near the sphere, which is accounted for separately. For small spheres, ξ less than 0.3, the approximation of *Rayleigh scattering* can be used.

3.7 RAYLEIGH SCATTERING:

Rayleigh scattering is important in the atmosphere where scattering is by gas molecules. Rayleigh derived the functional dependence by dimensional analysis and found that the scattered energy is proportional to $G^2(\tilde{n})V^2/\lambda_m^2$, where V is the volume of the particle and $G(\tilde{n})$ is the function of complex refractive indices of the scattering material and the surrounding medium. The important result is that for Rayleigh scattering, the scattered energy in any direction is proportional to the inverse fourth power of the wavelength of the radiation. This inverse dependence shows that when the incident radiation covers a radiation spectrum, the shorter-wavelength radiation will be Rayleigh scattered.

Rayleigh scattering by molecules of the atmosphere accounts for the background of the sky being blue and for the sun becoming red in appearance at sunset. The blue portion of the incident sunlight is at the short-wavelength end of the visible spectrum and hence it undergoes a strong Rayleigh scattering into all directions, giving the sky its overall blue background. Without molecular scattering, the sky would appear black except for the direct view of the sun.

3.8 MIE SCATTERING:

When scattering particles are not very large as explained in the sections above Rayleigh scattering and are not small enough to fall into the range adequately described by Rayleigh scattering, *Mie scattering theory* explains the nature of scattering in this range. This approximate range in which Mie scattering occurs is $0.3 < \xi < 5$.

Gustov Mie originally applied electromagnetic theory to derive properties of electro magnetic field when a plane spectral wave is incident on a spherical surface across which the optical properties change abruptly. Energy absorption by the medium, absorption by the scattering particles or both can be accounted for, and the results apply over the entire range of particle

diameters. Mie scattering is not strongly wavelength dependent and produces the almost white glare around the sun when a lot of particulate matter is present in the air.

Source: Thermal Radiation Heat Transfer, Third Edition, Siegel and Howell.

3.9 HEAT EXCHANGE AT WATER SURFACE

The heat exchange between air and water interface occurs in various different forms. This section of appendix primarily focuses in discussing these different methods of heat transfer with the help of figures attached at the end. All natural bodies dissipate heat to the atmosphere by back-radiation, evaporation, and conduction, while receiving heat primarily through short-wave solar radiation and long-wave atmospheric radiation. The physical processes influencing the heat transfer at the air water interface is shown in Figure 7.

The approximate ranges of magnitude of average daily values for the energies gained and lost at the air-water interface at mid-latitudes are shown in Figure 8. They comprise of short-wave solar radiation (H_s); long wave atmospheric radiation (H_a); long wave back radiation (H_b); heat loss or gain due to evaporation due to evaporation or condensation (H_e); reflected solar and atmospheric radiation (H_{sr} and H_{ar}), and loss or gain by conduction (H_c)

.

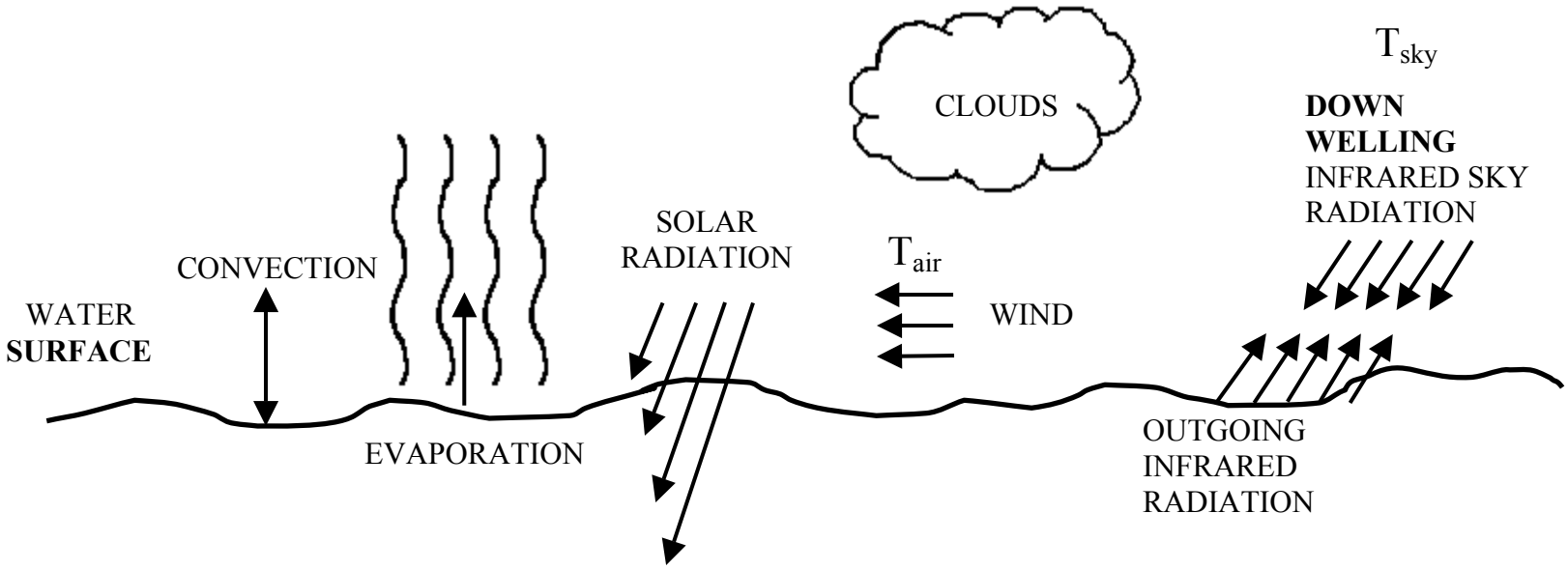

FIGURE 7 - PHYSICAL PROCESSES INFLUENCING AN AIR-WATER INTERFACE

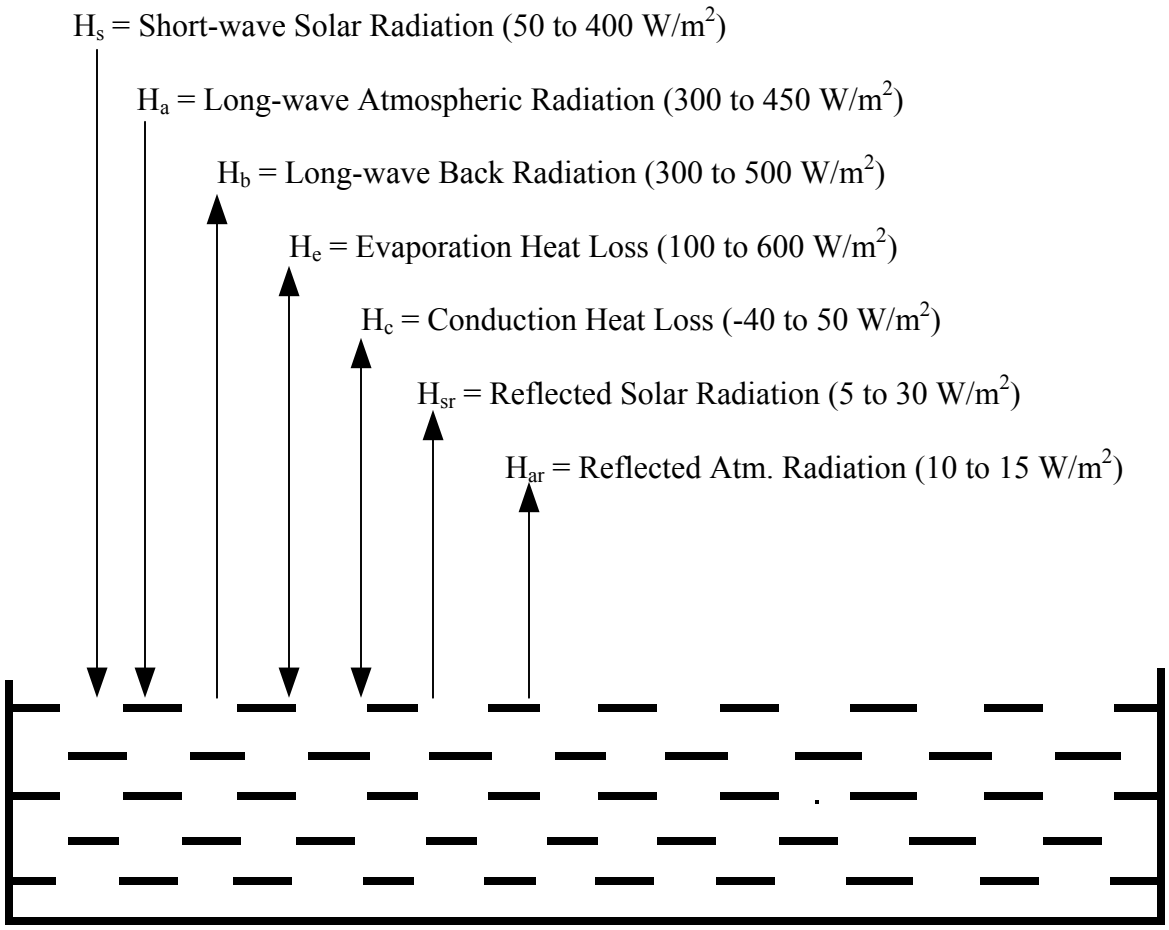

NET RATE AT WHICH HEAT CROSSES WATER SURFACE IS THUS CALCULATED AS:

$$\Delta H = (H_s - H_{sr} + H_a - H_{ar}) - (H_b \pm H_c \pm H_e)$$

{Independent of water surface temperature}

{Terms dependent on water surface temperature}

FIGURE 8 - PROCESSESS OF HEAT EXCHANGE AT NATURAL WATER SURFACE

3.9.1 Short Wave Solar Radiation (H_s):

The incoming solar energy is in the form of short-wave radiation, which passes directly from the sun to the earth through the earth's atmosphere. About 99% of the short-wave solar radiation is contained in a wavelength range between 0.14μ and 4.0μ with the maximum intensity at about 0.5μ.

The intensity of short-wave radiation reaching the earth's atmosphere is calculated from the "solar constant" which is defined as the flux of solar radiation at the earth's outer atmosphere received on a surface normal to the sun's direction at the earth's mean distance from the sun. Its value is 1390 W/m^2. The intensity of radiation received on any portion of the earth's atmosphere varies with latitude on the earth, time of day, and season of the year. The amount of short-wave solar radiation reaching the surface of the earth depends on what happens to the short-wave radiation as it passes through the earth's atmosphere, where it will be depleted by many factors. The most important factors are (*a*) absorption by ozone in the upper atmosphere, (*b*) scattering by dry air, (*c*) absorption, scattering, and diffuse reflection by suspended matter, and (*d*) absorption and scattering by water vapor.

Many researchers in the past have discussed different methods for computing the short-wave solar radiation reaching the surface of the earth. The Lake Hefner Report (Marciano and Harbeck, 1952) [Appendix B] discusses and evaluates two empirical formulae, which may be used to compute solar radiation. Mosby and Raphael give the solar radiation as a function of cloud cover and sun's altitude. Kennedy's formula gives the clear sky solar radiation at the exterior of the earth's outer atmosphere, an atmospheric transmission coefficient and the ratio of the length of the actual path of the solar beam to the path through the Zenith.

3.9.2 LONG WAVE ATMOSPHERIC RADIATION (H_A):

The long wave radiation from the atmosphere ranges in wavelength between 4μ and 120μ and has its peak intensity at about 10μ. Atmospheric radiation depends primarily on air temperature and humidity and increases as the moisture content of air increases. It constitutes the major thermal input to a water body at night and on warm cloudy days. In some heat studies, its magnitude has been computed by using the fourth-power law and a constant emissivity of about 0.87.

However, atmospheric radiation does not follow a simple law. It is a function of many variables, notably the distributions of moisture, temperature, ozone, carbon dioxide, and other atmospheric constituents. The magnitude of the long wave radiation may be estimated by use of empirical formulae, which accounts for some of these variables. Brunt's formula (Marciano and Herbeck, 1952) gives values that are usually within about 15% of measured values. The graph for Brunt's coefficient is shown in Figure 9.

$$H_a = 4.4 \times 10^{-8} (T_a + 273)^4 [C_a + 0.031(e_a)^{0.5}] \ (W/m^2) \qquad (A.1.1)$$

where

T_a is the air temperature (C) measured about 2 m above the water surface,

e_a is the air vapor pressure (mm Hg) at the same location, and

C_a is Brunt's coefficient, which may be determined from the air temperature and the ratio of the measured solar radiation to clear sky solar radiation. The latter ratio can be developed approximately by dividing the total daily solar radiation (calculated by integrating the pyrheliometer solar radiation curve) by the approximate value of the clear sky radiation curve.

.

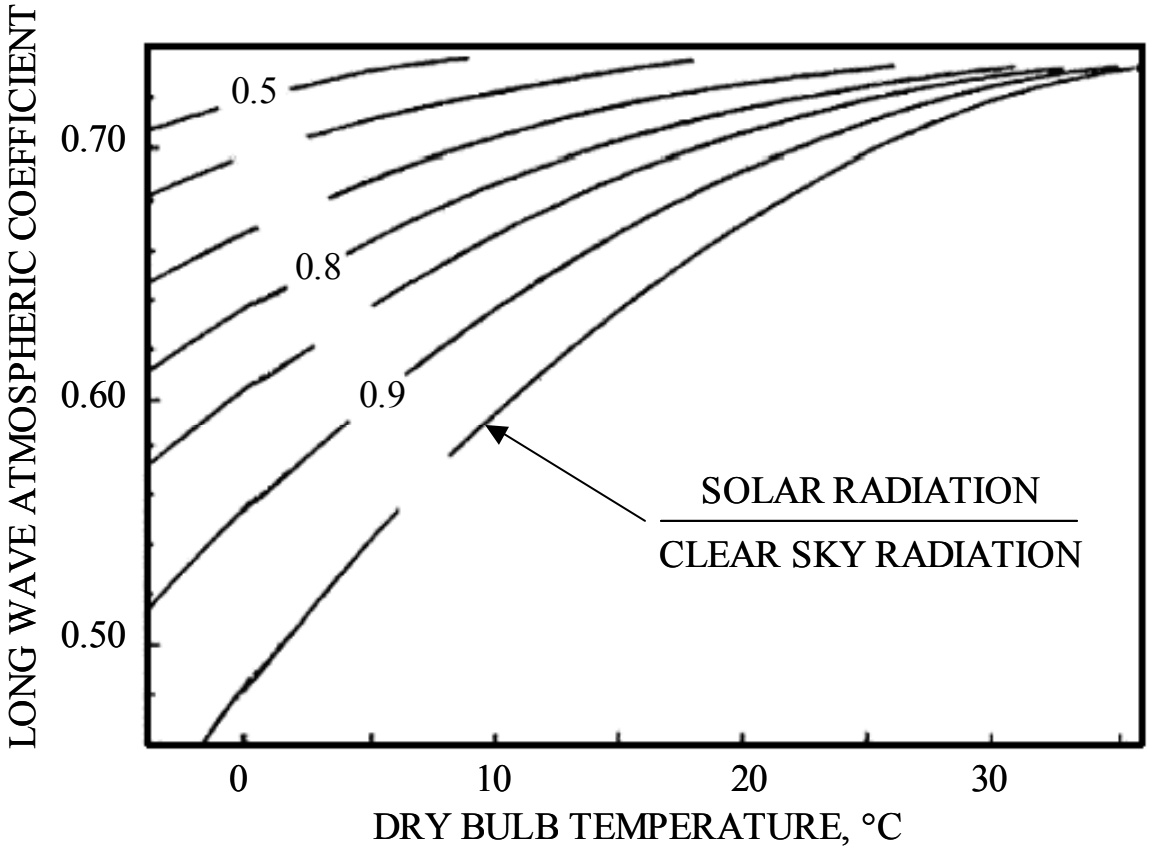

FIGURE 9 - BRUNT'S COEFFICIENT

3.9.3 REFLECTED SOLAR AND ATMOSPHERIC RADIATION (H_{SR} AND H_{AR}):

The fractions of the solar and atmospheric radiant energies that are reflected from the water surface may be calculated using their respective reflectivity coefficients, which are ratios of reflected radiation to the incident radiation, viz:

$R_s = H_{sr} / H_s$, where R_s is the solar reflectivity

$R_a = H_{ar} / H_a$, where R_a is the atmospheric reflectivity

The solar reflectivity, R_s, is more variable than the atmospheric reflectivity, R_a. The former is a function of the sun's altitude and the type and amount of cloud cover while the later is relatively constant at about 0.03.

3.9.4 LONG WAVE BACK RADIATION (H_B):

Long wave back radiation is the radiation energy that is emitted by water back to the atmosphere as long waves in the wavelength range from 4μ to 120μ. Figure 8 indicates that this long wave back radiation accounts for a substantial portion of the heat loss from a body of water. Since water radiates as an almost perfect black body, the rate at which heat is lost by back radiation, H_b, can be computed from Stephen-Boltzman fourth-power radiation law as:

$$H_b = \varepsilon \sigma (T_e + T_s)^4 \ (W/m^2) \qquad (A.1.2)$$

where

ε is the emissivity of water ($\varepsilon = 0.97$),

σ is the Stephen-Boltzman constant ($\sigma = 5.67 \times 10^{-8}$ W m^{-2} K^{-4})

T_e is the water surface temperature (C)

T_s is the absolute temperature of zero C which is equal to 273.15 K

3.9.5 CONDUCTION HEAT LOSS OR GAIN (H_C):

Heat can enter or leave the water by conduction if the air temperature is greater than and less than the water temperature. As Figure 8 explains, the daily average rate of heat conduction is an order of magnitude less than other terms in the heat balance of the air-water interface. The rate at which heat is conducted between the two media is proportional to the temperature difference between the two media, which is given as:

$$H_c = C_0 (T_s - T_a) \quad \text{(A.1.3)}$$

where,

C_0 is the conduction heat transfer coefficient that depends on the wind speed.

T_s, T_a represents the water surface temperature and air temperature respectively.

Bowen (1926) has defined the conduction heat transfer coefficient, C_0 defined above as a function of wind speed defined by

$$C_0 = C_c f(W) \quad \text{(A.1.4)}$$

where C_c is Bowen's coefficient, which is empirically found to be approximately 0.47 mm Hg/C. Combining equations A.1.3 and A.1.4 yields:

$$H_c = 0.47 f(W) (T_s - T_a) \ (W/m^2) \quad \text{(A.1.5)}$$

3.9.6 EVAPORATION (H_E):

Evaporation energy is the heat lost from a body of water to the atmosphere. Each kilogram of water (at 20C) that leaves as water vapor carries away its latent heat of vaporization of 5.85×10^5 cal (2.45×10^6 J). Again, the water body regains an exact same amount of heat when the water vapor in the atmosphere condenses as water and enters the water body. The later phenomenon happens rarely, usually at night, if the water temperature falls below the dew point temperature.

There are many methods of estimating evaporation. Most of them are empirical. There have been some attempts to derive evaporation formulae from the basic principles of fluid mechanics. Among these studies, the work of Sverdrup (1937) is notable. The Lake Hefner study [Appendix B] was setup explicitly to develop an empirical formulation for evaporation in terms of meteorological variables, and the water budget approach was used as a direct measure of evaporation.

A general evaporation formula gives the rate of evaporation as a function of the wind speed and the difference between the saturated water vapor pressure at water surface temperature and the water vapor of the overlying air, thus:

$$H_e = f(W)\ (e_s - e_a)\ (W/m^2) \qquad (A.1.6)$$

and

$$f(W) = a_0 + a_1 W + a_2 W^2\ (W\ m^{-2}\ mm\ Hg^{-1}) \qquad (A.1.7)$$

where

W is the wind speed (m/s),

e_a is the air-water pressure (mm Hg) and

e_s is the saturation vapor pressure of the air adjacent to the water surface (at temp T_s).

CHAPTER 4: PROPOSED ENERGY BALANCE MODEL

4.1 CONDUCTION ZONE

The air-water interface is thought to have three distinct thermodynamic zones and associated gradients as illustrated in Figure 10. Each zone is characterized by the primary means for heat movement. Radiation dominates from the surface down to about 20 μm. This "radiation zone" is the origin of conventional radiometric sea surface temperature (SST) readings. Due to the thinness of the layer, a practical way of measuring the surface (skin) temperature without disturbing the layer is via infrared thermometry. The "conduction zone" is identifiable by the linear gradient characteristic of conductive processes. Most of the temperature difference between the surface and the bulk near surface water temperature is found in the top millimeter. The temperature deviation in this zone is negative under most circumstances (that is, the surface is cooler than the water a few millimeters below). The difference in water temperatures in this zone drives the conductive heat transfer process. When multiplied by water thermal conductivity, this gradient is a measure of total heat flux from the water to the atmosphere. This heat flux is the main energy input to atmospheric circulation. It is returned to the atmosphere at the same or different location (i.e. after transport by ocean currents) in the form of long wave radiation and turbulent heat fluxes. Thus a large portion of the energy driving atmospheric circulation has to cross the ocean's boundary layer (Grassl, 1976). Below the conduction zone heat moves primarily by turbulent eddy diffusion (McKeown, 1995). The resulting temperature becomes constant in this layer.

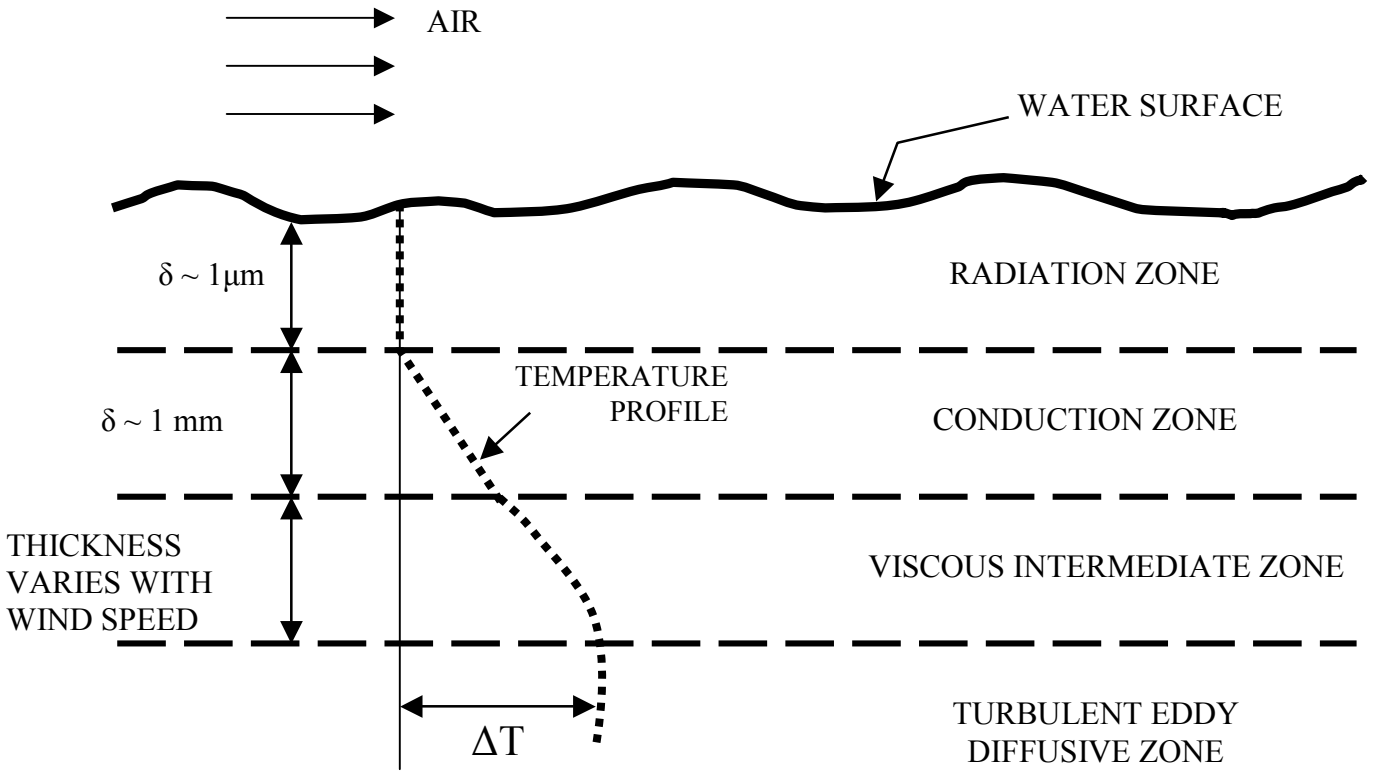

FIGURE 10 - THERMODYNAMIC AIR-WATER INTERFACE ZONES

The conduction zone gradient is most useful because a conduction heat flux can be calculated from the conduction zone gradient, that is

$$Q_{cond} = k\frac{(T_w - T_s)}{\delta}$$

where

δ is the conduction zone thickness [m]

k is the thermal conductivity of water [W / (m – K)]

T_w is the bulk water temperature [K]

T_s is the water surface temperature [K]

4.2 SOLAR ENERGY RADIATION

The solar energy incident on the surface of the earth is considered to consist of direct and diffuse parts as shown in Figure 3. The part of solar radiation that reaches the earth's surface without being scattered or absorbed by the atmosphere is called direct solar radiation, Q_D. The scattered radiation is assumed to reach the earth's surface uniformly from all the directions and is called diffuse solar radiation, Q_d. Then the total solar energy incident on a unit area of a horizontal surface is

$$Q_{solar} = Q_D Cos\theta + Q_d$$

where θ is the angle of incidence of direct solar radiation (i.e. the angle that the sun's rays make with the normal to the surface). The diffuse radiation varies from about 10 percent of the total radiation on a clear day to nearly 100 percent on a totally cloudy day (Cengel, 1998).

4.3 CLOUD COVER

The effect of cloud cover on the solar radiation (as shown in Figure 11) may be estimated by the following parabolic relationship (Raphael, 1962)

$$Q_{solar/cloud} = \left(1 - 0.0071C^2\right)Q_{solar}$$

where C is the average cover in tenths of sky covered (e.g. C = 10 for 100% cloud cover). Cumulus and Stratocumulus clouds are usually the dominant depleters of solar radiation (Garrett, 1997).

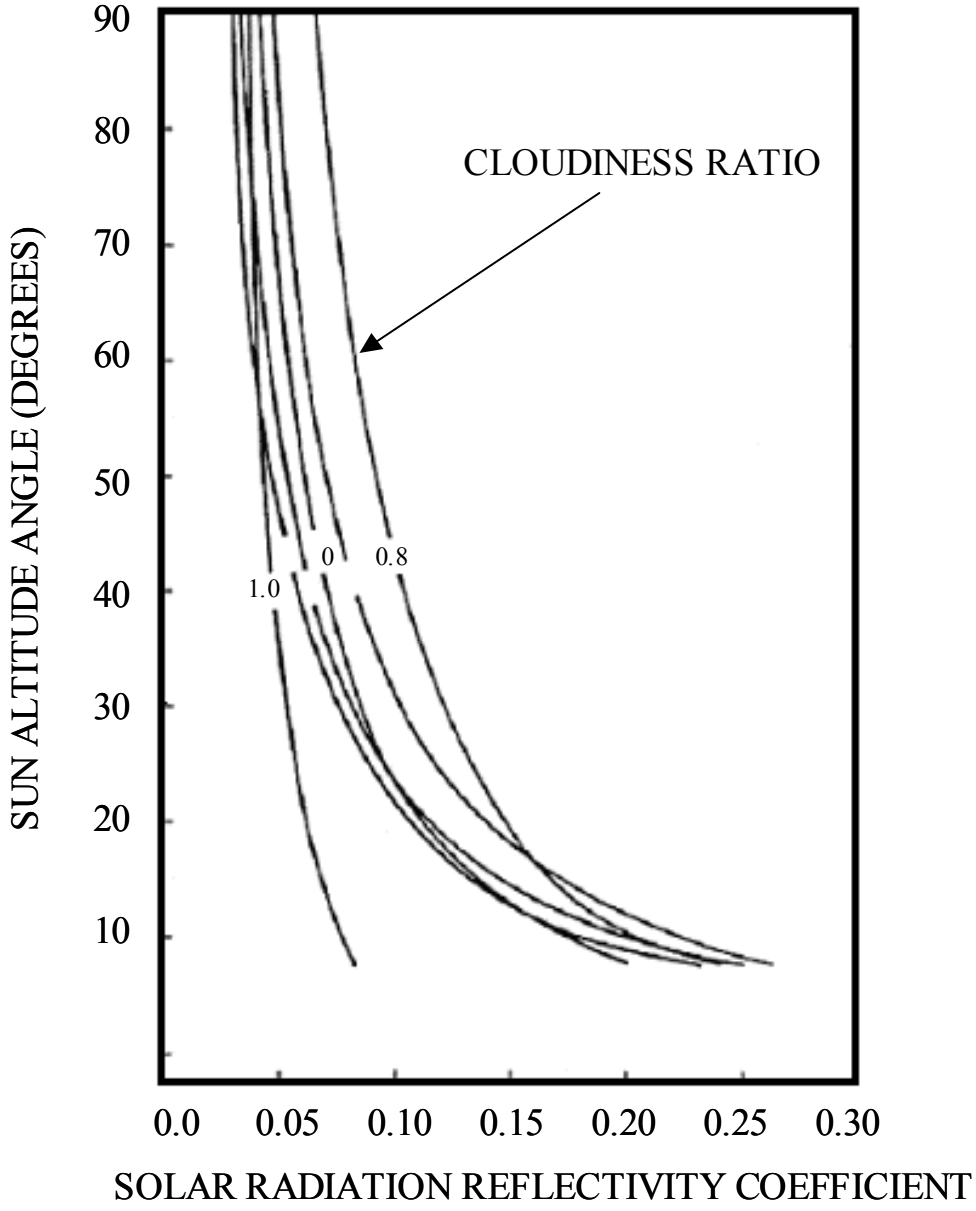

FIGURE 11 - REFLECTIVITY OF SOLAR RADIATION

4.4 SOLAR ENERGY ABSORPTION IN WATER

The spectral distribution of solar energy striking the surface of the earth is shown in Figure 5. The long wavelength, (i.e. infrared) is absorbed at the surface of the water; whereas, the shorter wavelengths (i.e. visible and ultraviolet) penetrate into the water column and transfer heat into the water below the skin. Depending on the amount of suspended matter in the surface layer the short wave radiation may be absorbed within the upper few centimeters (highly turbid coastal waters) or extend down tens of meters in clear waters (Suhluessel, et al, 1990). During the day under low wind conditions solar heating warms up the upper meters of a pond creating an afternoon temperature maximum a few millimeters below the surface. At night vertical mixing erases this maximum creating a continuously increasing temperature profile below the surface (Suhluessel, et al, 1990).

The fractions of solar radiation transmitted through a water column in various spectral intervals in given in Table 1 by Siegel and Howel (1992) and Kondratyev (1969). Also the fraction of solar radiation absorbed in various water layers is shown in Table 2. It can be observed from either of the tables that the absorption of solar radiation by the water column as it passes through it cannot be described by a simple exponential because different wavelengths vary widely in their absorption coefficients. The short wavelengths penetrate tens of meters, whereas, the near infrared is absorbed within the first few millimeters or centimeters.

Spectral Interval 8μm	Incident Solar energy Distribution	Fraction of energy transmitted through various water-layer thickness, cm							
		0.1	1	2.5	10	50	100	1000	10000
0.3-0.6	0.237	0.237	0.237	0.237	0.236	0.233	0.229	0.173	0.014
0.6-0.9	0.360	0.359	0.353	0.332	0.305	0.227	0.129	0.010	
0.9-1.2	0.179	0.172	0.123	0.072	0.008	0.004			
1.2-1.5	0.087	0.063	0.017	0.009					
1.5-1.8	0.080								
1.8-2.1	0.025								
2.1-2.4	0.025	0.001							
2.4-2.7	0.007								
TOTALS	1.000	0.859	0.730	0.650	0.549	0.464	0.358	0.183	0.014

TABLE 1 - FRACTION OF SOLAR RADIATION SPECTRUM TRANSMITTED THROUGH VARIOUS THICKNESS OF WATER.

Spectral Interval 8μm	Incident Solar-energy Distribution	Fraction of energy absorbed in a water-layer thickness, cm							
		0-0.1	0.1-1	1-2.5	2.5-10	10-50	50-100	100-1000	≥1000
0.3-0.6	0.237	0.000	0.000	0.000	0.004	0.013	0.169	0.024	0.730
0.6-0.9	0.360	0.003	0.017	0.058	0.075	0.217	0.272	0.331	0.028
0.9-1.2	0.179	0.039	0.274	0.285	0.358	0.022	0.022		
1.2-1.5	0.087	0.276	0.529	0.092	0.104				
1.5-1.8	0.080	0.663	0.337						
1.8-2.1	0.025	1.000							
2.1-2.4	0.025	0.096	0.004						
2.4-2.7	0.007	1.000							
TOTALS									
0.3-2.7	1.000	0.141	0.129	0.080	0.101	0.085	0.106	0.175	0.183

TABLE 2 - FRACTIONS OF SOLAR RADIATION SPECTRUM ABSORBED IN VARIOUS WATER LAYERS

The angle of incidence, θ, of the direct sunlight varies with the time of day and year according to the formula

$$\text{Cos } \theta = \text{Cos L Cos D Cos } (2t/24) - \text{Sin L Sin D}$$

where

t = time in hours (noon = 0)

L = latitude

D = D (t) = declination of the sun

$$\text{Sin D} = 0.4 \text{ Cos } (2d/365)$$

d = time in days, measured from June 21.

This introduces two complications because the reflective losses increase with an increase in the angle of incidence and because the light has to travel a factor of 1/cos r farther to penetrate to a given depth of a pond, r = angle of refraction in degrees. Table 3 lists the angle of refraction, the reflective loss, and the factor 1/cos r for various angles of incidence, θ, for water with a refractive index n = 1.33.

Angle of Incidence	Angle of Refraction	Reflective loss	1/cos r
0	0.00	0.020	1.00
10	7.50	0.020	1.01
20	14.90	0.020	1.04
30	22.08	0.021	1.08
40	28.90	0.024	1.15
50	35.17	0.033	1.23
60	40.63	0.059	1.32
70	44.95	0.133	1.41
80	47.77	0.347	1.49
90	48.75	1.000	1.52

TABLE 3 - ANGLE OF REFRACTION R, REFLECTIVE LOSS, AND 1/COS R FOR VARIOUS ANGLES OF INCIDENCE

4.5 SOLAR RADIATION RELATION AS A FUNCTION OF TIME OF DAY

A simple relationship for solar radiation flux as a function of time of day is a sinusoidal variation and is given as:

$$Q_{solar} = 950 \text{ Cos } (2\pi t/24)$$

where, t is the time in hours with t = 0 corresponding to solar noon. The amplitude of 950 corresponds to the average value of the solar radiation reaching the earth's surface on a clear day (Cengel, 1998). Also, the following Figure 12 shows mean solar radiation distribution as a function of month of the year. The graph below can be used to read the average solar radiation energy in [W/m^2].

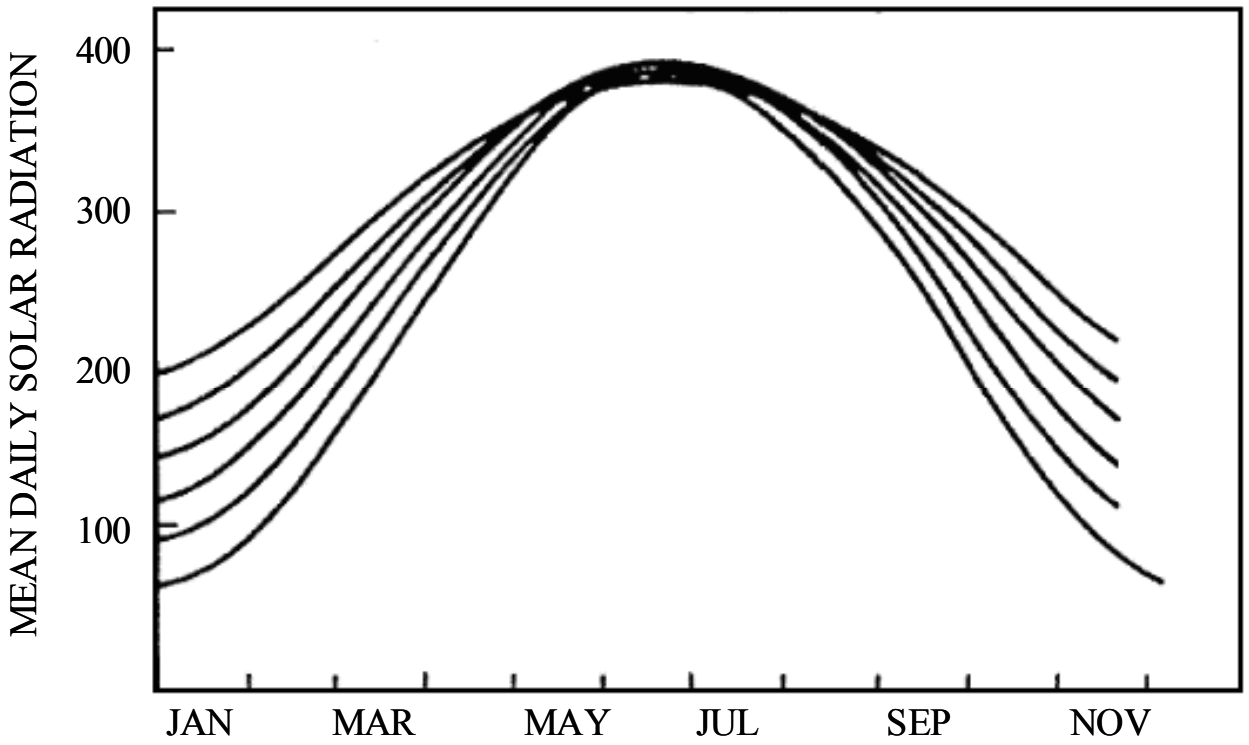

FIGURE 12 - MEAN DAILY SOLAR RADIATION AS A FUNTION OF MONTH

4.6 SKY RADIATION

The sky radiation is caused due to the presence of gas molecules and suspended particles in the atmosphere as shown in Figure 4. The absorption and emission of radiation caused by gases such as N_2, H_2, and O_2 are negligible but larger molecules such as H_2O and CO_2 have a significant role in the sky radiation. This radiation depends primarily on the humidity and air temperature and increases as the moisture content of the air increases. It constitutes the major input to a body of water on warm cloudy days and at nights (Edinger, et al, 1974). This long wavelength radiation is completely absorbed at the surface of water. Although the atmospheric emission is far from resembling the distribution of radiation from a black body, it is found convenient in radiation calculations to treat the atmosphere as a black body at some lower fictitious temperature that emits an equivalent amount of radiation energy. This fictitious temperature is called effective sky temperature, T_{sky}. The radiation emission from the atmosphere to the earth's surface is then expressed as

$$Q_{sky} = \sigma T_{sky}^4$$

The value of T_{sky} ranges from about 230 K for cold, clear-sky conditions to about 285 K for warm, cloudy-sky conditions (Cengel, 1998).

Since the effective sky temperatures does not deviate much from the ambient temperature, thus, in light of kirchoff's law, the absorptivity of a surface can be taken to be equal to its emissivity, i.e., $\alpha = \varepsilon$. Then the sky radiation absorbed by the surface can be expressed as

$$Q_{sky\ absorbed} = \alpha Q_{sky} = \alpha \sigma T_{sky}^4 = \varepsilon \sigma T_{sky}^4$$

The spectral emissivity of the ocean's surface varies sharply between 3 and 200 μm with values of 0.95 near 11 μm and 0.75 near 100 μm (Schluessel, et al., 1990). Using refractive index

values from Downing and Williams (1975) effective emissivities of 0.886 at 280 K and 0.891 at 300 K for a flat-water surface were computed.

An alternative approach to calculate the atmosphere radiative emission without the need for estimating T_{sky} is as follows. The emission may be written in terms of T_{air} and ε_{sky}, that is

$$Q_{sky} = \varepsilon_{sky} \sigma T_{air}^4$$

The emissivity of the sky, ε_{sky}, is given by Berdahl and Fromberg (1982) and Mills (1999) for a clear sky as

Day: $\varepsilon_{sky} \approx 0.727 + 0.0060\ T_{dew}$ (° C)

Night: $\varepsilon_{sky} \approx 0.741 + 0.0062\ T_{dew}$ (° C)

where T_{dew} is the dew point temperature in degrees centigrade. These expressions are based on data obtained at a number of locations in United States. The dew point generally changes little in any 24-hour period (Edinger, et al., 1974). Table 4 shows a list of day and night sky emissivities at different dew point temperatures.

In solar energy applications, the spectral distribution of incident solar radiation is very different than the spectral distribution of emitted radiation by a surface, since the former is concentrated in the short-wavelength region and latter is in the infrared region. Therefore, the radiation properties of surfaces cannot be assumed to be grey. Instead, the surface is assumed to have two sets of properties: one for solar radiation and another for infrared radiation at ambient temperature (Cengel, 1998).

T_{dew} (^{o}C)	Sky Emissivity	
	Day	Night
5	0.757	0.772
10	0.787	0.803
15	0.817	0.834
20	0.847	0.865
25	0.877	0.896
30	0.907	0.927
Average	0.832	0.850

TABLE 4 - SKY EMISSIVITY

4.7 SKY RADIATION / CLOUD COVER

Anderson (1954) conducted an exhaustive study (reviewing nearly two centuries of research) of the effects of cloud cover on sky radiation and developed the following relationships considering vapor pressure p_v, in mbar, cloud cover, C in tenths of sky covered, and cloud height H, in feet

$$\underline{Q_{sky}} = \beta = a + b\, p_v$$

$$\sigma\, T_{air}^{4}$$

where

$$a = 0.740 + 2.5\, C\, e^{-0.0584H}$$

$$b = 0.0049 - 0.054\, C\, e^{-0.06H}$$

Anderson (1954) stated

"The range is least, and the effect of vapor pressure is greatest, for clear skies over the entire vapor pressure range; the effect of vapor pressure decreases as the cloud amount increases. For any given amount of cloud cover, the radiation increases over the entire vapor pressure range as the height of the clouds decreases. The modification of the radiation, from the clear sky case, is least for high scattered clouds and greatest for low overcast. For low overcast, the radiation is independent of vapor pressure."

Anderson (1954) concluded that the above equations were valid with 10% accuracy. Most weather observations give cloud cover without regard to cloud height, H; therefore, Anderson (1954) modified his work to produce Figure 13 depicting β as a function of cloud cover C and vapor pressure, p_v, only. This graph may be approximated by the following equation for computation purposes

$$Q_{sky/clouds} = (0.80 + 0.0000385 p_v)\, Q_{sky}$$

where the vapor pressure, p_v, is expressed in Newtons/meter^2 (pascals).

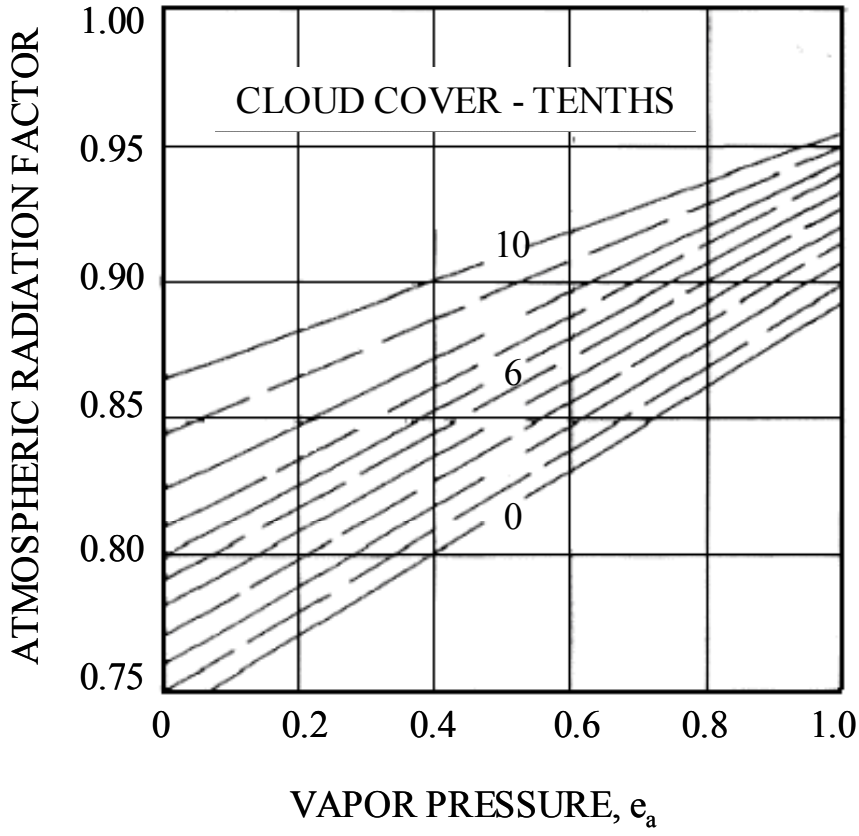

Atmospheric Ration Factor, $\beta = \dfrac{Q_a}{\sigma T_a^4}$

FIGURE 13 - ATMOSPHERIC RADIATION FACTOR AS A FUNCTION OF VAPOR PRESSURE AND CLOUD COVER

4.8 CLOUDS

Clouds have a pronounced influence on the earth's energy balance yet the formation of cloud cover is still very difficult. As noted previously clouds have an important effect on both sky and solar radiation. Clouds may be treated as blackbodies (emitters and absorbers) in the infrared because they contain condensed water in the form of ice crystals or cloud droplets that are excellent infrared absorbers (Shaw, 2000). Table 5 explains the effects of different types of clouds.

Type	Description	Area Covered	Effects on Solar Radiation
Stratus	Low-lying, dense, surface to 2 km	Large	Efficient reflector, albedo = 0.5
Cumulus	Convectively active, separate puffs forms storm clouds, 2 to 7 km	Localized	Efficient reflector, albedo = 0.5
Cirrus	High, thin ice, 5 to 13 km	Large	Inefficient reflector, albedo = 0

TABLE 5 - EFFECTS OF CLOUDS

Clouds scatter solar radiation and control earth's albedo (i.e., the fraction of the incident solar energy that is reflected back to space). Earth's planetary albedo is calculated to be about 0.33. It depends on the numerous factors such as the distribution of clouds, snow and ice, pollution, aerosols, dust, ocean spray, crops, etc. Clouds cover about 60% of the earth's surface at any given time (Shaw, 2000). Clouds help to diffuse radiation via multiple scattering.

The top of the clouds are much colder than the bottom, thus the emission to the top is less intense than the radiation from the bottom of the cloud; therefore high level clouds (e.g., Cirrus) produce a net warming; whereas, low level clouds produce a net cooling effect. Overall, the global effect of clouds is to produce a small net cooling of the Earth's surface (Shaw, 2000). The structure of the atmosphere is explained well in Table 6.

Name	Height (km)	Temperature Range (K)
Troposphere	0-10	290-220
Stratosphere	10-47	220-270
Mesosphere	47-79	270-180
Thermosphere	>79	180-210

TABLE 6 - STRUCTURE OF THE ATMOSPHERE

4.9 WATER SURFACE TEMPERATURE

Figure 14 summaries the process of interaction that can take place between rays of electromagnetic energy and the atmosphere, as they affect what is observed in the field of view of a sensor (Robinson, 1997). Ray 1 represents the useful signal i.e. radiation leaving the water surface which reaches the sensor, containing the information about the water temperature. Ray 2 represents the radiation leaving the water, which is absorbed by the atmosphere *en route*, whilst Ray 3 is that which is scattered by the atmosphere out of the sensor field of vision. The sum of 1,2, and 3 represents the energy, which is received by the sensor if a complete correlation is to be made between the received signal and the water temperature. The absence of 2 and 3 from reaching the sensor must therefore be allowed for in some form of atmospheric correction to the received data. In addition, rays 4, 5, and 6 reach the sensor without having left the sea surface in the field of view, and therefore constitute extraneous noise on top of the signal. Ray 4 is that energy emitted by the constituents of the atmosphere, which is a function of temperatures at different altitudes. Ray 5 is the energy reflected by scattering into the field of vision of the sensor, and Ray 6 is a special case of scattering into the field of vision-energy which has previously left the sea-surface but from outside the field of view. Ray 1 may of course be represent energy which has been forward scattered, provided it originally left the sea surface within the field of view. The total energy that arrives at a sensor is integrated over the view path from contributions at each altitude. The resultant distribution does not particularly resemble that of a blackbody at a single temperature but it is a mixture of black bodies over a range of temperatures. Moreover, radiation from lower altitudes is absorbed and re-emitted at higher altitudes, making the situation more complicated (Schowenger, 1999).

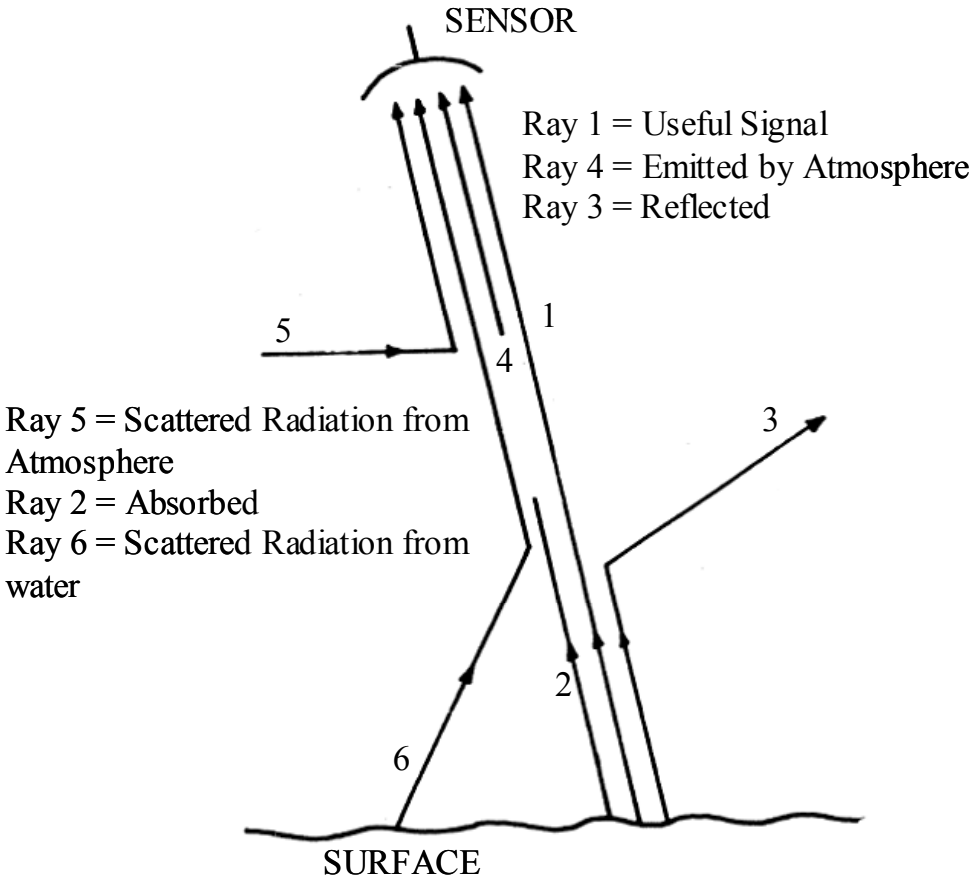

FIGURE 14 - SATELLITE SENSOR MEASUREMENT

Thus the radiance incident on a radiometer directed at a water surface may be given by

$$Q_{water} = \int \{\varepsilon(\lambda) P(\lambda, T) + (1 - \varepsilon(\lambda)) Q_{sky}\} d\lambda$$

where $p(\lambda, T)$ is Planck's function. The atmospheric emission, absorption, and scattering is neglected due to the very short path between the radiometer and water.

In practice water surface temperatures are usually made in the infrared wavelength window between 8μm and 14 μm. This is most useful for earth observation work for several reasons. It encompasses the radiant energy peak at 9.5 μm for a black body at 300 K which is near the earth's ambient temperature; also, most of the incident direct solar energy around 9.5 μm is absorbed by the ozone layer. Transmission of the water temperature energy is quite high over the entire 8-14 μm window, and the window is spectrally very broad permitting integration over a sizable fraction of the total distribution (Schott, 1977).

In practice, most sensors integrate over a spatial region and measure a weighted average radiance, which is then related to the equivalent black body temperature through a calibration curve.

4.10 EVAPORATION

In the atmosphere, the continuous evaporation and condensation of water from the soil, oceans, and lakes influence every form of life and provides many of the day-to-day varieties of climate that govern the environment on earth. These processes are very complicated because in practice they are governed by substantial atmospheric convection currents that are difficult to describe analytically (Holman, 1996). Evaporation occurs when liquid molecules near the surface experience collisions that increase their energy above that needed to overcome the surface binding nature. When water evaporates into the air heat energy is removed in two ways. The most important heat removal is through the energy required to change the phase of water

from a liquid to vapor. The secondary heat loss is by the physical removal of energy contained in the water removed by evaporation (Raphael, 1962). For example, an average size swimming pool can lose 5 m^3 (~ 1000 gallons) of water per month due to evaporation (Schultz, 2002). The energy associated with the phase change is the latent heat of vaporization of the liquid. The energy required to sustain the evaporation must come from the internal energy of liquid, which then must experience a reduction in temperature. However, if steady state conditions are to be maintained, energy transfer to the liquid from the surroundings must replenish the latent energy lost by the liquid because of evaporation. The transfer may be due to solar radiation or convection of sensible energy from air. Evaporation is the second largest component (next to shortwave radiation) in a sea-air energy budget (Zhang and McPhaden, 1995). It should be noted that the above mentioned latent heat may be regained by water by condensation but this happens only rarely, usually at night, if the water temperature falls below the dew-point temperature (Edinger, et al, 1974).

4.11 CONVECTION

Convection heat transfer between the water surface and the air may be conveniently expressed in terms of long term average wind speed by an empirical relation given by McAdams (1954).

$$Q_{conv} = (5.7 + 3.8V)\,(T_s - T_{air})$$

where V is the wind speed in m/s, T_s is the surface water temperature, and T_{air} is the air temperature in degrees K.

The American Society of Heating, Refrigeration and Air Conditioning Engineers (ASHRAE, 1982) recommends another simple formulae for heat loss from swimming pool in terms of temperature difference only

$$Q_{loss} = 107(T_{water} - T_{air})$$

This equation apparently includes convection, advection, and radiation as well as evaporation heat losses. Typical average values for such parameters as wind speed, relative humidity, heat transfer coefficient, etc. has most likely been utilized to obtain the coefficient of "107". The ASHRAE document does not clarify this point.

4.12 ENERGY BALANCE ANALYSIS

An energy analysis of the heat and mass transfer mechanisms existing at an air-water interface leads to the following energy balance at the surface, that is,

Energy to the interface = Energy from the interface

or

$$\alpha_s Q_{solar} + \alpha Q_{sky} + Q_{cond} = Q_{conv} + Q_{evap} + Q_{water} + Q_{advected}$$

where

Q_{solar} is the incoming solar radiation (both direct and diffuse),

Q_{sky} is the radiant energy from the sky,

Q_{cond} is the energy received from the water by conduction,

Q_{conv} is the convective energy to/from the air,

Q_{evap} is the evaporation from the water to the air, and

$Q_{advected}$ is the energy loss of the evaporated water mass.

Substituting the heat fluxes from the appropriate equations into the above equation,

$$\alpha_s(Q_D \text{ Cos } \theta + Q_d) + \varepsilon\, Q_{sky} + k(T_w - T_s)/\delta = h(T_s - T_{air}) + Q_{evap} + \varepsilon\, \sigma\, T_s^4 + Q_{advected}$$

where all the temperatures are in degrees Kelvin. The water emissivity, ε, absorptivity, α, are taken to be equal since the sky temperatures is not significantly different than the water surface temperature. McAlister and McLeish (1969) not that sky radiation in the longer wavelengths (i.e., infrared) is largely emitted from the lower atmosphere, where the temperature is seldom

much below water temperature. They further note that changes in wavelength distribution of the sky radiation appears to have only a limited effect on heat transfer. The equation above may be rearranged in a more conventional form to give

$$\alpha_s(Q_D \text{ Cos } \theta + Q_d) = k(T_s - T_w)/\delta + h(T_s - T_{air}) + \varepsilon\sigma(T_s^4 - T_{sky}^4) + Q_{evap} + Q_{advected}$$

which indicates that the solar heating is balanced by the conduction, convection, radiation, and evaporation.

It is interesting to note that studies of heat budgets averaged over several years have shown that the heating of the earth's surface by sky radiation (long wave) is greater than that from the solar radiation (short wave) by a factor of approximately two (Edinger, et al, 1974).

The next chapter discussed the results of energy balance approach by analyzing the equation shown above using real-time data from field experiments.

CHAPTER 5: RESULTS AND CONCLUSION

This chapter discusses the results of all the six models discussed in Chapter 2 and the energy balance model discussed in Chapter 3 with the help of experimental data.

5.1 LAKE HEFNER EVAPORATION MODEL

The evaporation energy equation as explained in Chapter 2 is as follows:

$$E_p = (e_0 - e_a) * (0.42 + 0.0040 u_p)$$

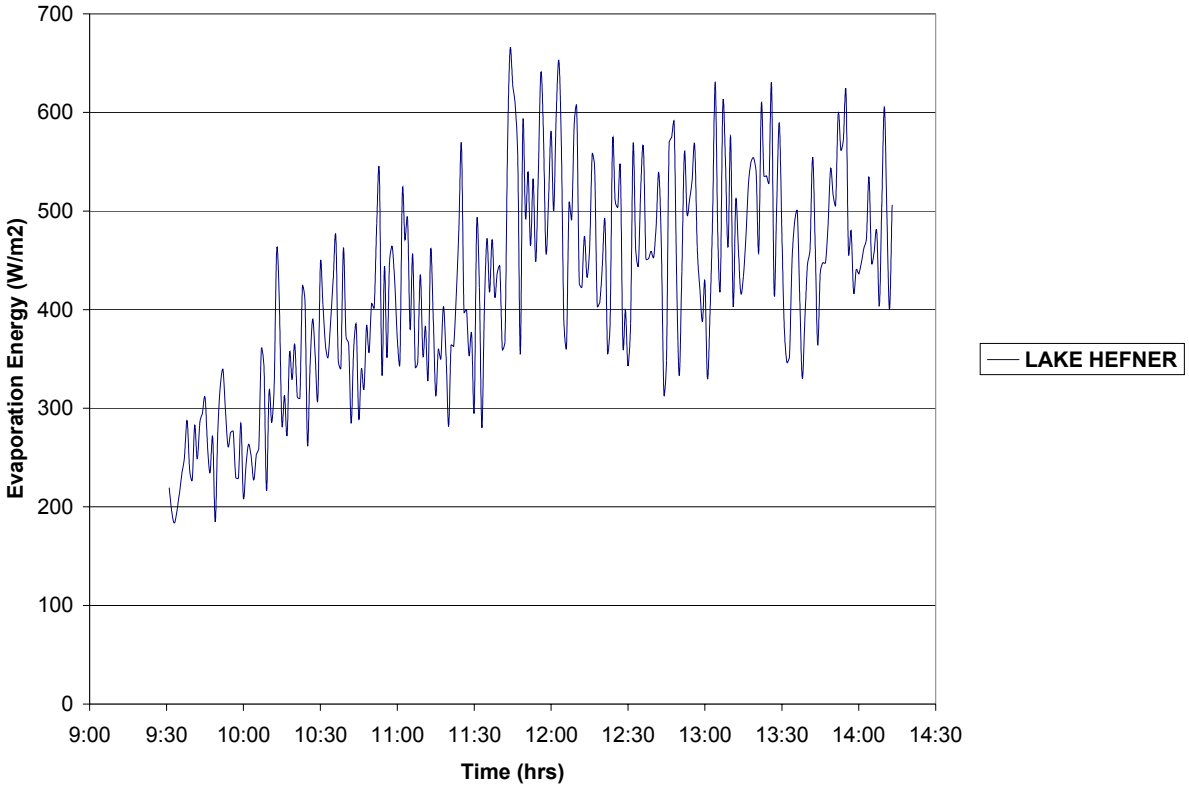

The graph indicated an increase in the evaporation energy with the time of the day, which can be explained as follows: The vapor pressure difference increases with the time of the day because the saturation vapor pressure increases with the time of the day. The fluctuations in the graph can be attributed to the velocity term in the above equation. The wind velocity data was measured every two seconds and averaged every minute.

5.2 JP HOLMANS EVAPORATION FORMULA – IN VAPOR PRESSURES

JP Holman's empirical experimental evaporation formula (in inches/day)

$$E' = 0.8(0.37 + 0.0041u)(p_s' - p_w')^{0.88}$$

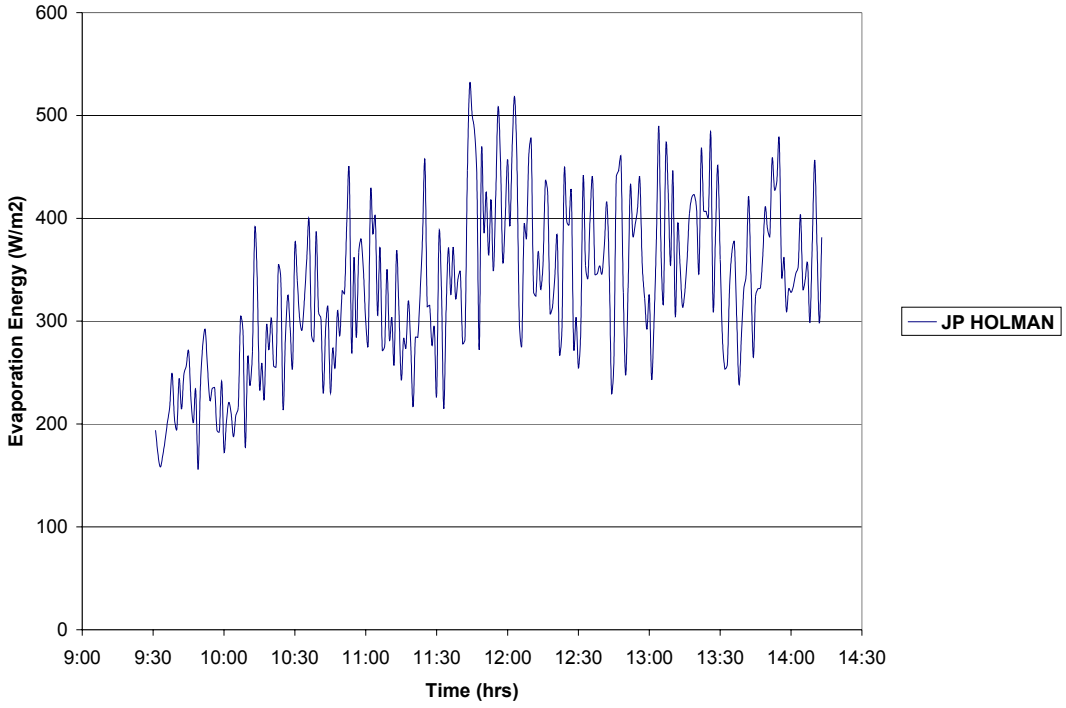

As observed in the previous model, J.P. Holman's evaporation equation also shows a trend similar to Lake Hefner evaporation model. The magnitude of evaporation energy in this model is lower than the previous model.

J.P. Holman's model has a pan coefficient of 0.8 as shown in the equation above. The pan coefficient is used to correct the evaporation measured in evaporation pans to an actual water body evaporation such as a lake. A coefficient of 0.7 is used for terrestrial or land evaporation and 0.8 for lakes and reservoirs. Similar to the previous model, the evaporation increases with the time of the day and the fluctuations are due to the velocity term in the equation.

5.3 JP HOLMAN'S FORMULA MODIFIED USING AMBIENT TEMPERATURE

JP Holman's formula modified by writing vapor pressure in terms of Ambient Temperature (Hall and Mackie, 2000) and converting inputs into SI system, the resultant formula for evaporation (in W/m^2)

$$E = 0.45(0.37 + 0.22V)(5T_{air}^{2} - 51T_{air} + 1282)^{0.88}(1-\Phi)^{0.88}$$

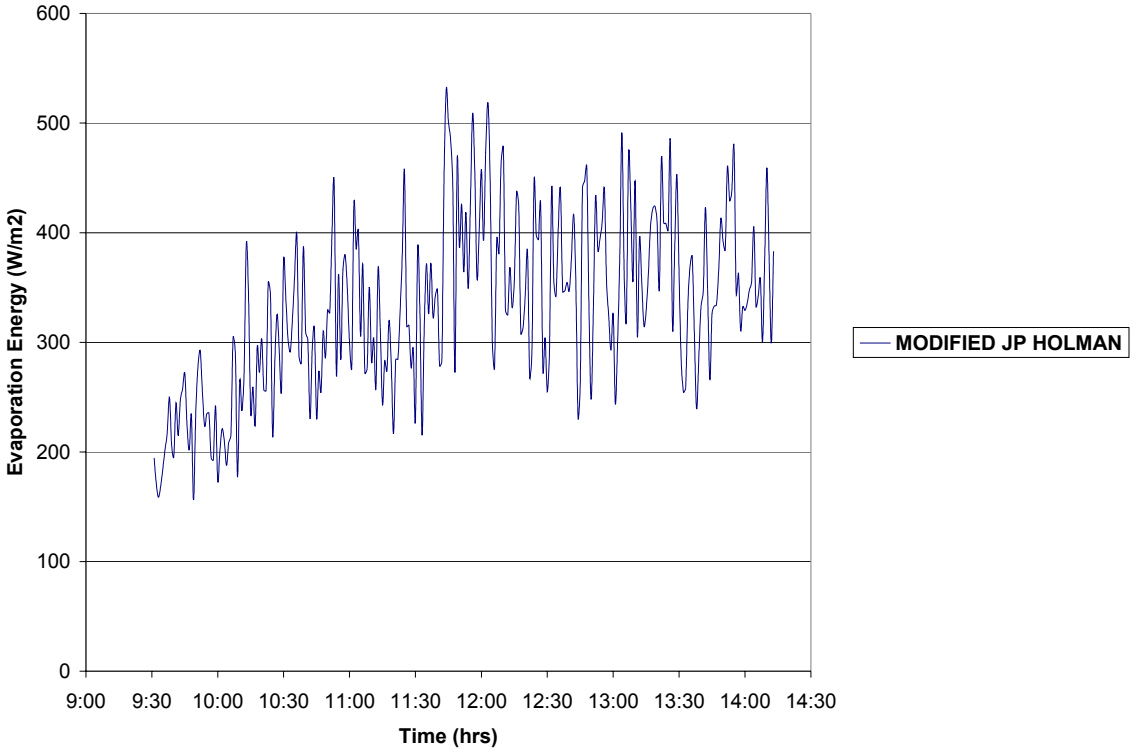

The above equation is much more practical to use than the original evaporation equation due to the fact that ambient temperature can be more directly than vapor pressure. The evaporation energies measured by the current and the original J.P. Holman methods are very similar. The evaporative energy increases with time of the day. The magnitudes of evaporation energies are also very similar.

5.4 EPRI MODEL – REPORT NO.14 – EVAPORATION MODEL

Evaporation equation prepared for Electric Power Research Institute, Report no.14 (Edinger et al) in W/m^2 is given as,

$$E = (9.2 + 0.46W^2)(e_s - e_a)$$

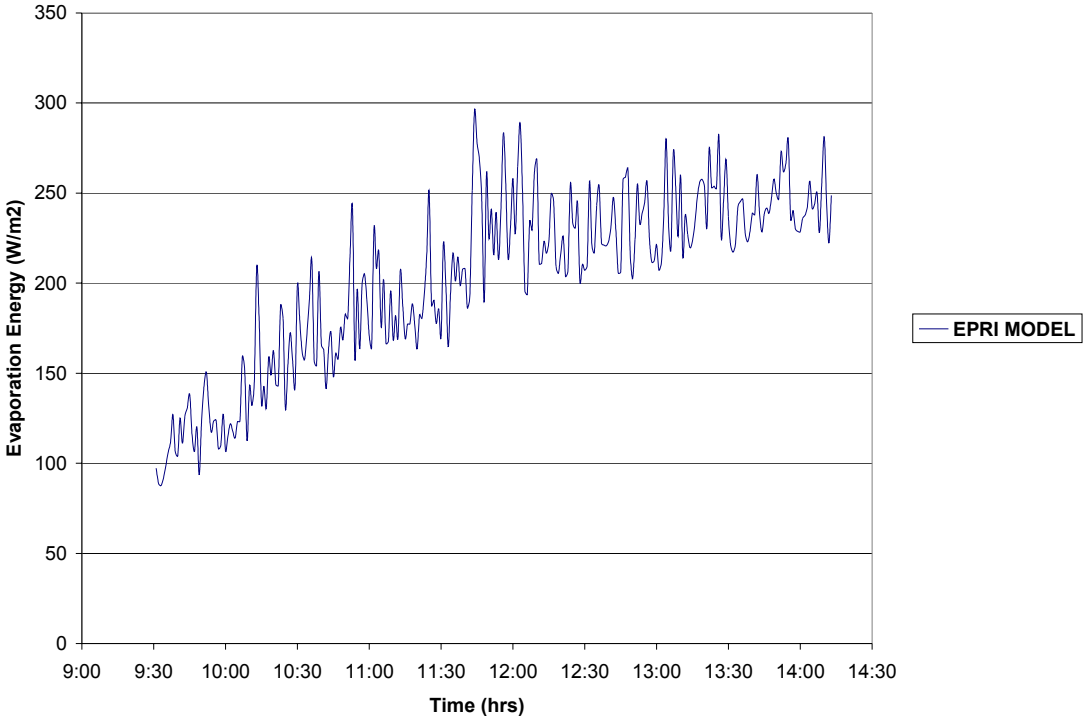

A major difference between the current model and all the other models studied earlier is that the evaporative energy is proportional to the square of velocity term instead of velocity term directly. The effect of this relationship can be observed by the fact that the fluctuations in the evaporation energy are lower compared to the earlier models. Another important observation is that the magnitude of evaporation energies is significantly lower than the earlier models. The reason for this behavior can be attributed to the constants with which the wind velocity term is multiplied.

5.5 EVAPORATION EQUATION FROM SOLAR ENGINEERING FOR DOMESTIC BUILDINGS

Evaporation losses from pools as given by Himmelman (in W/m^2),

$$Q_{evap} = 9.15K_E(e_s - e_a)$$

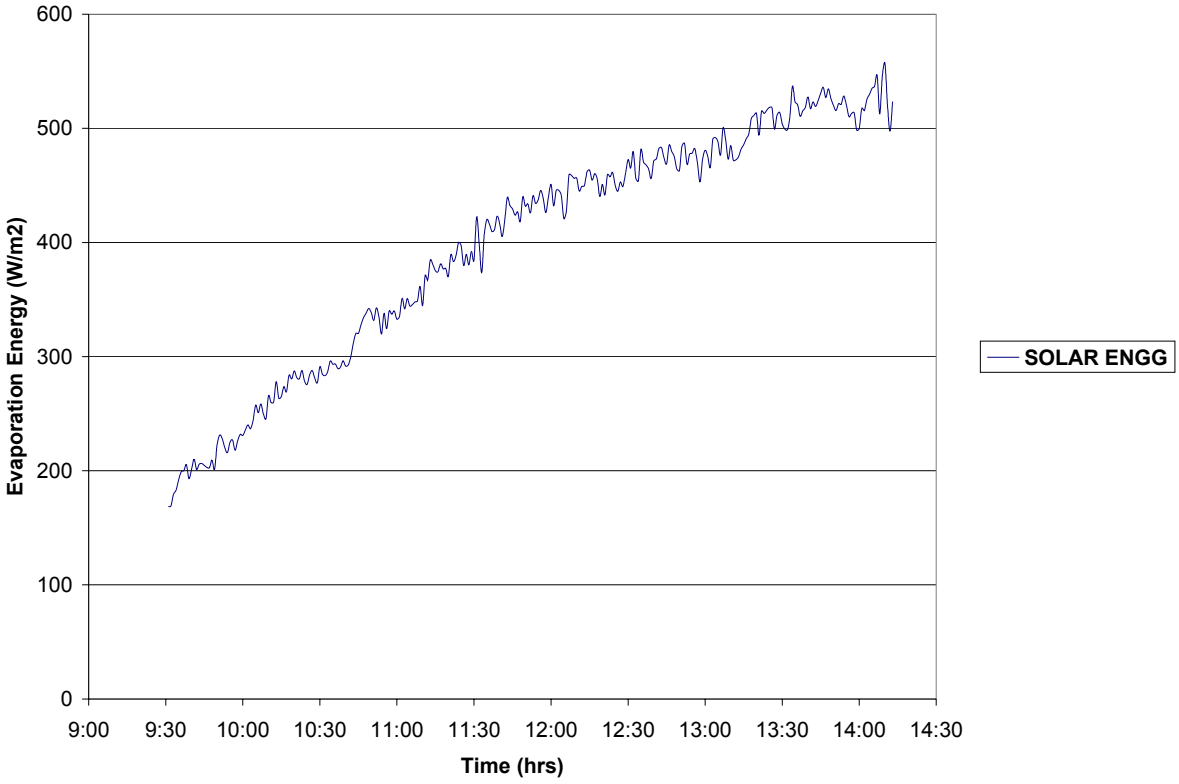

The evaporation equation provided by Solar Engineering is a function of vapor pressure difference only and is completely independent of the wind velocity term. This equation assumes a constant overall heat transfer coefficient of 60 $W/m^2.°C$. The graph shows fewer fluctuations for not considering wind velocity in the equation. The magnitude of evaporation energy is similar to Lake Hefner and Holman's energy equations.

5.6 ASHRAE HANDBOOK, 1999

Heat Loss from a pool surface in Btu/hr.ft^2 is given as,

$$Q_{evap} = W*U*(T_p - T_a)$$

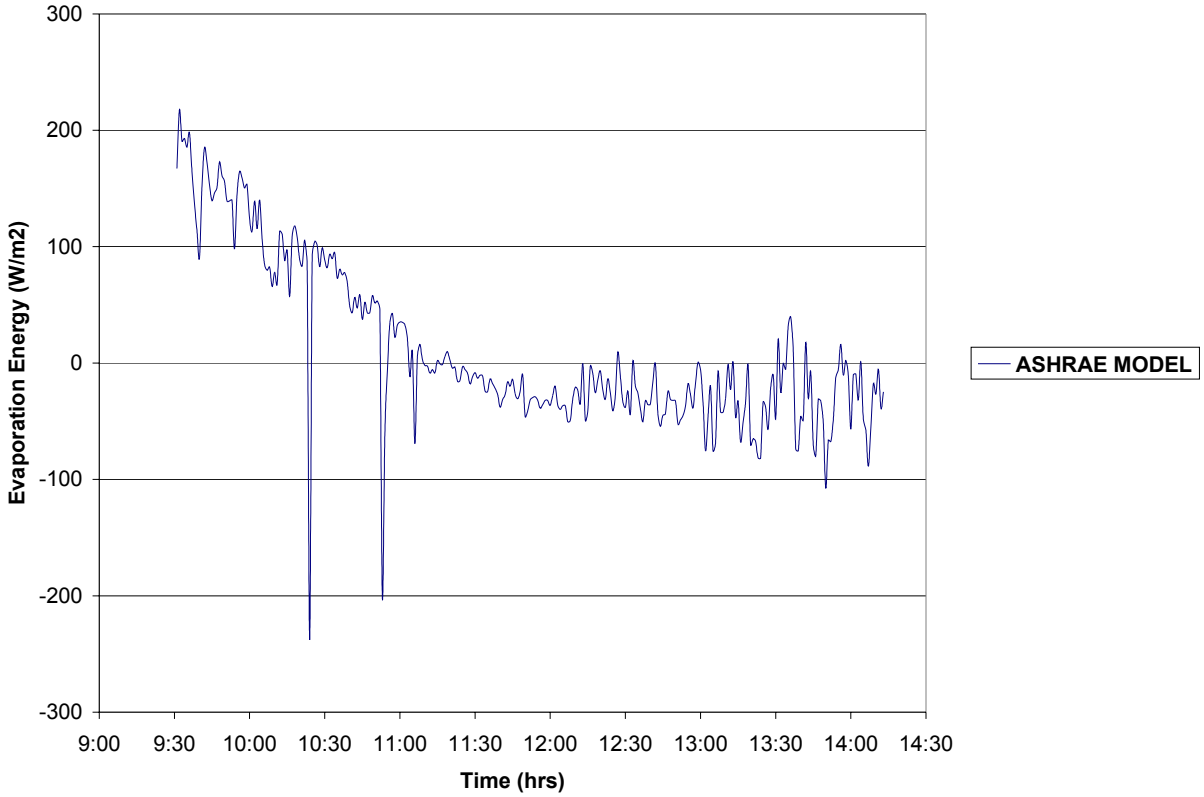

A.S.H.R.A.E evaporation model has a very different energy equation. The evaporation energy is defined as a function of temperature difference between water surface and ambient air. The graph shows a decreasing trend of evaporation energy with time. This is an error caused by considering evaporation as a function of temperature delta only. In reality, even when the water surface temperature is lower than air temperature, evaporation can still occur if air is dry i.e., low relative humidity and in the presence of wind. The spikes on the curve are due to measurement errors due to a change in the sensor position.

5.7 ENERGY BALANCE MODEL

Energy into the water body = Energy from the water body

$$\alpha s Q solar + \varepsilon sky Q sky + Q cond = Q conv + \mathbf{Q_{evap}} + Q water + Q advected$$

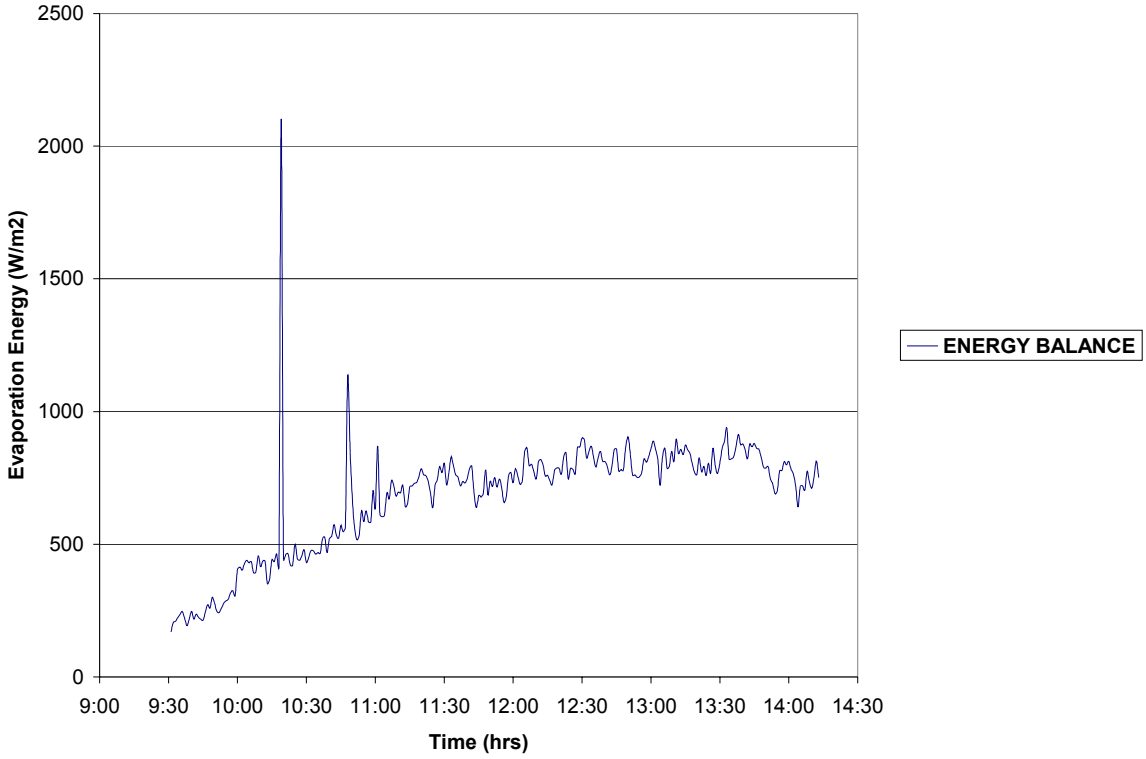

This graph represents the energy balance model prediction for evaporation energy in W/m^2. The magnitude of evaporation energy calculated by the proposed model is higher than any other model discussed earlier. The spikes on the curve are due to the errors in the measurement data similar to the previous model. The proposed model is more accurate than any of the models discussed earlier for the following reasons:

1. Shows an increase in the evaporative energy with time of day which is expected
2. Lesser fluctuations even after considering wind velocity factor
3. Sensitive to the delta T term in the equation proven by the spikes on the curve

5.8 COMPARISON OF ALL MODELS

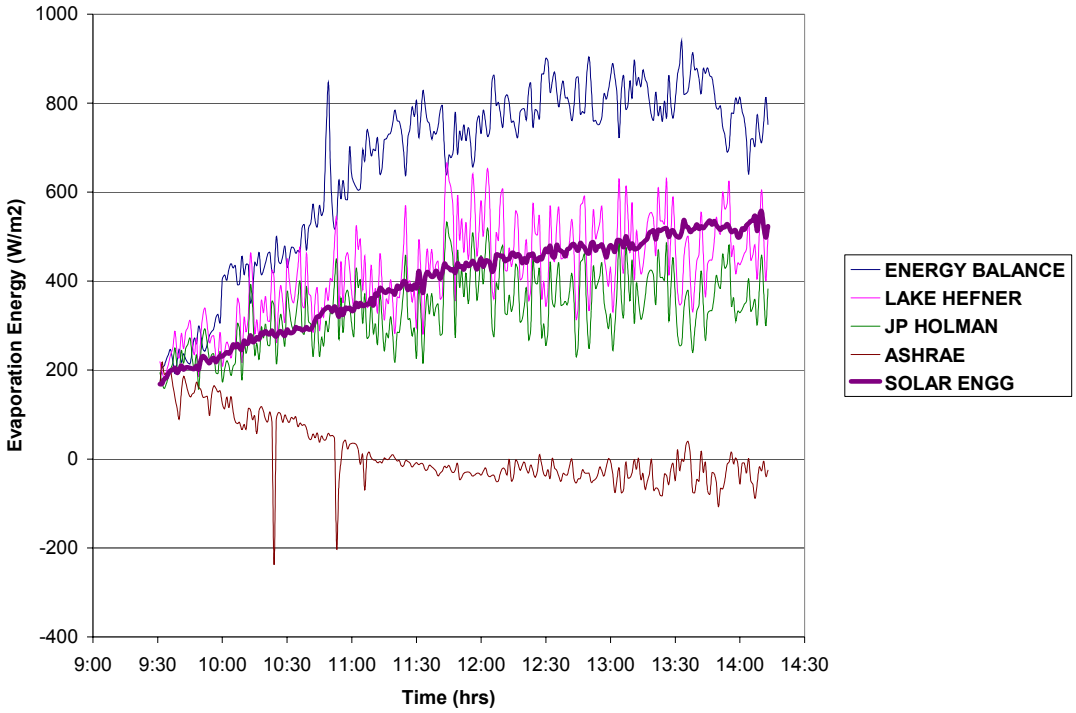

The graph shown above shows a quick comparison of various models studied in this chapter including the proposed energy balance model. The graph shows that an energy balance model predicts a higher evaporation than any other evaporation model discussed in this chapter. It is interesting to observe a large variation predicted by various models. There is not a lot of real data available to confirm the accuracy of any one of the above-mentioned models. The scope of the current study ends here with the following recommendations for future work:

1. A need for more study and research in this area.
2. Understand conductive heat transfer
3. Study overall heat transfer coefficient
4. Study advection energy
5. Need for more experimental evaporation data

REFERENCES

1. American Society of Heating, Refrigerating, and Air Conditioning Engineers, ASHRAE Applications, 1982 and 1991.
2. Anderson, E.R., 1954, Energy-Budget Studies, *Water Loss Investigations: Lake Hefner Studies, Professional Paper 269,* Geological Survey, U.S. Department of Interior, Washington, D.C., pp. 71-119.
3. Berdahl, P. and Fromberg, R., 1982, The Thermal Radiance of Clear Skies, *Solar Energy*, vol. 29, pp. 299-314.
4. Burt, W.V., 1958, Heat Budget Terms for Middle Snake River Reservoirs, *Technical Report No. 6*, Reference 58-7, School of Science, Oregon State College, Corvallis, Oregon, December.
5. Cengel, Y.A., 1998, *Heat Transfer: A Practical Approach,* WCB/McGraw-Hill.
6. Downing, H.D. and Williams, D., Optical Constants of Water in the Infrared, *Journal of Geophysical Research,* Vol. 80, pp. 1656-1667, 1975.
7. Edinger, J.E., Brady, D.K. and Geyer, J.C., *Heat Exchange and Transport in the Environment,* Electric Power Research Institute, EPRI Publication No. 74-049-00-3, November, 1974, John Hopkins University, June, 1965.
8. Ewing, G. and McAlister, E.D., 1960, On the Thermal Boundary Layer of the Ocean, *Science*, N.Y. 131, 1374.
9. Garrett, A.J., August 11, 1997, *ALGE: A 3-D Thermal Plume Prediction Code for Lakes, Rivers and Estuaries,* Savannah River Technology Center, DOE, SRTC-NN-95-25, Rev. 1.

10. Grassl, H., 1976, The Dependence of the Measured Cold Skin of the Ocean on Wind Stress and Total Heat Flux, *Boundary-Layer Meteorology,* Vol. 10, pp. 465-474, Reidel Publishing, Holland.
11. Hall, C.A., and Mackie, June, 2001, C., Semi-analytic Solutions for Freezing Induced by Evaporative Cooling, International Journal of Heat and Mass Transfer, Pergamon, pp. 1161-1170.
12. Harbeck, G.E., 1969, Discussion of "The Cooling of riverside thermal-power plants". In Parker, F. and Krenkel, P., *Engineering Aspects of Thermal Pollution*, Vanderbilt University Press, Nashville, TN., pp. 133-143.
13. Holman, J.P., 1996, Heat Transfer, 8 th ed., McGraw-Hill, New York.
14. Incropera, F.P. and DeWitt, D.P., 1985, *Fundamentals of Heat and Mass Transfer*, 2 nd edition, John Wiley & Sons, New York.
15. Katsaros, K.B., 1980, The Aqueous Thermal Boundary Layer, *Boundary Layer Meteorology*, Vol. 18, pp. 107-127.
16. Kohler, M.A., Nordenson, T.J. and Fox, W.E., May, 1955, Evaporation from Pans and Lakes, *U.S. Department of Commerce Weather Bureau Research Paper 38*.
17. Kondratyev, Y.K., 1969, *Radiation in the Atmosphere*, Academic Press, N.Y.
18. Kreith, F. and Kreider, J.F., 1978, *Principles of Solar Energy*, Hemisphere Publishing, Washington.
19. McAdams, W.H., 1954, *Heat Transmission*, 3 rd edition, McGraw-Hill, New York.
20. McAlister, E.D., and McLeish, W., June 20, 1969, Heat Transfer in the Top Millimeter of the Ocean, *Journal of Geophysical Research*, Vol. 74, No. 13.

VITA

Ravi Praveen S Eluripati was born in Karimnagar, Andhra Pradesh, India. After attending primary and secondary high schools in various towns (mostly in the Telangana Region of Andhra Pradesh), he graduated high school in June 1993 from Singareni Collieries High School, Yellendu, Khammam district of Andhra Pradesh. He attended Muffakham Jah College of Engineering & Technology from July 1995 to June 1999 and graduated with a Bachelors of Engineering degree majoring in mechanical engineering. He entered University of New Orleans in pursuit of a master's degree in mechanical engineering in January 2000. He started his career as a mechanical engineer in January 2002 in General Electric Company (GE Power Systems) in Schenectady, NY and presently working in the Gas Turbine Technology division of GE Energy in Greenville, SC.